A STUDY OF VIBRATIONAL RELAXATION IN SHOCK HEATED SO_2, SO_2 + Ar AND SO_2 + He BY LASER SCHLIEREN TECHNIQUE

A Thesis Submitted
In Partial Fulfilment of the Requirements
for the Degree of
DOCTOR OF PHILOSOPHY

By
VALLENTYNE VINOD NIRANJAN KISHORE

to the

DEPARTMENT OF CHEMICAL ENGINEERING
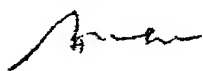
INDIAN INSTITUTE OF TECHNOLOGY KANPUR
JANUARY, 1978

CHE-1970-D-KIS-STU
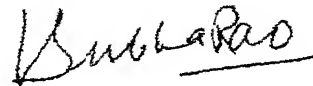
TO

MY FATHER

M.V. VALLENTYNE

CERTIFICATE

This is to certify that the work described in this thesis is the original work of Mr. V.V.N. Kishore performed under our supervision and has not been submitted elsewhere for a degree.

(S.V. Babu)
Asst. Professor
Department of Chemical Engineering
Indian Institute of Technology
Kanpur

(V.Subba Rao)
Professor
Department of Chemical Engineeri.
Indian Institute of Technology
Kanpur

ACKNOWLEDGEMENTS

I thank Veena for her efficient handling of the situation in the crucial last hours. I thank Mr. M.M. Beg for his efficient typing of the manuscript.

V.V.N. KISHORE

TABLE OF CONTENTS

LIST OF FIGURES

LIST OF TABLES

ABSTRACT

Name of student	:	V.V.N. Kishore
Programme	:	Ph.D.
Department	:	Chemical Engineering
Title of the thesis	:	A study of vibrational relaxation in shock heated SO_2, SO_2+Ar and SO_2+He by laser schlieren technique
Supervisors	:	Dr. V.Subba Rao
		Dr. S.V. Babu
		Department of Chemical Engg.
Institute	:	Indian Institute of Technology Kanpur-208016, India

Vibrational relaxation times are measured in pure SO_2, SO_2-Ar and SO_2-He mixtures using a shock tube - laser schlieren technique. The temperature ranges covered have been 550 - 1200°K for pure SO_2, 700 - 2100°K for SO_2-Ar mixtures (11% SO_2, 20% SO_2 and 54% SO_2 in Argon) and 700 - 1600°K for SO_2-He mixture (9.5% SO_2 in Helium). All the measurements are made on incident shock waves. The schlieren signals obtained in SO_2 and SO_2-Ar and SO_2-He mixtures have been found to exhibit a double exponential behaviour. The fast decay times could not be measured accurately and only the longer relaxation times are reported. The following equations are obtained to describe the temperature dependence of the relaxation times.

$$(P\,\tau)_{SO_2-SO_2} = \exp\,(-2.965 + 11.9\ T^{-1/3}) \qquad (700-2100°K)$$

$$(P\,\tau)_{SO_2-Ar} = \exp\,(-4.65 + 40.32\ T^{-1/3}) \qquad (700-2100°K)$$

$$(P\,\tau)_{SO_2-He} = \exp\,(-7.58 + 54.68\ T^{-1/3}) \qquad (700-1600°K)$$

INTRODUCTION

When a gaseous system under thermodynamic equilibrium
is suddenly disturbed by an external perturbation, the system
reattains equilibrium through molecular collisions in which
energy is exchanged among the various degrees of freedom of
the molecular components. The translational and rotational
degrees equilibrate quite rapidly while the vibrational deg-
rees are known to lag behind. The mechanism by which the vi-
brational degrees of a molecular system attain equilibrium
is known as vibrational relaxation. The energy transfer proce-
sses by which the energy of the gas molecules is distributed
among the various vibrational levels fall into two categories:
i) V-T/R and ii) V-V energy transfer processes.

In a V-T/R process the energy is transferred from the
vibrational degrees to the translational/rotational degrees or
vice-versa due to molecular collisions. An example of such a
process is

$$O_2 \ (v=1) + O_2 \ (v=0) \longrightarrow O_2 \ (v=0) + O_2 \ (v=0) + \triangle E$$
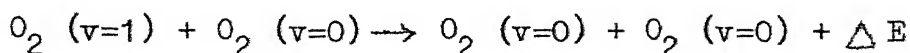
In this process an oxygen molecule in the vibrational state
v=1 (where v is the vibrational quantum number) looses its

vibrational energy upon collision, and this loss of energy is accompanied by an increase in the translational/rotational energy of the colliding molecules.

In a V-V energy transfer process, the loss of one or more vibrational quanta in one molecule is accompanied by the simultaneous gain of vibrational quanta in the other colliding molecule and the difference in the vibrational energies exchanged is accounted by a change in the translational/rotational energies of the colliding pair. Some examples of this kind of processes are

$$SO_2(2\nu_2) + SO_2(0) \rightleftharpoons SO_2(0) + SO_2(\nu_1) - \triangle E = 120 \ cm^{-1}$$

$$CO_2(0) + N_2(v=1) \rightleftharpoons CO_2(\nu_3) + N_2(v=0) - \triangle E = 18 \ cm^{-1}$$
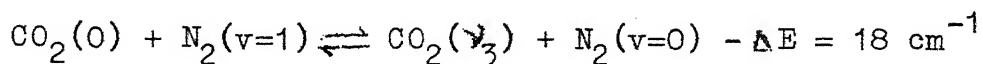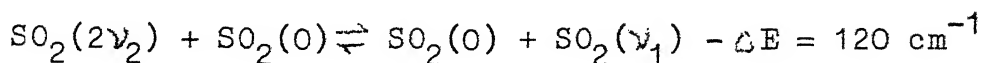
Knowledge of the rates of these vibrational energy relaxation processes is of great importance for many reasons. It can be said that an essential preliminary to the understanding of reaction kinetics is the detailed understanding of vibrational energy transfer since in many cases vibrational relaxation is the first step in the chemical activation or deactivation of molecules. Further, since the advent of powerful infrared gas lasers, vibrational energy transfer studies have acquired particular significance because of the need, both for further development in laser research and for

a comprehensive understanding of the processes occuring during
laser operation. On the more practical side, the thrust of a
rocket motor or other type of high intensity combustion devices
will depend on the internal state of the combustion products
and a knowledge of relaxation rates is desirable for optimal
design. On the other hand, a variety of theories are being put
forward to make 'a priori' calculations of the vibrational
energy transfer rates and an accurate measurement of these
rates will serve to check the validity of the various theories.

A variety of experimental techniques are available for
quantitative measurements of relaxation rates. Some of the
well established methods are: i) ultrasonic methods, ii) laser
induced fluorescence technique, iii) shock tube methods, etc.

The ultrasonic technique makes use of the fact that
the speed of a sound wave depends on the specific heat ratio,
γ . At sufficiently low sound frequencies the normal values
for the specific heats will apply, but at high frequencies
there will not be enough time for the internal energy of the
molecules to change. Thus at high frequencies the specific
heat will effectively be reduced and the speed of sound will
be higher. From measurement of the sound frequency at which
this velocity change occurs the relaxation time can be cal-
culated. Measurements on both ultrasonic absorption and

dispersion are commonly used for the estimation of relaxation times. These techniques as well as the results for various molecules are well reviewed[1,2]. This method can not be used in practice at high temperatures (above 1000°K), and it does not give any information about high frequency molecular vibrations which make a relatively small contribution to the specific heat. However, this method has proved to be extremely useful for measurements on lowlying vibrational states at low temperatures.

In the laser induced fluorescence technique, a strong vibrational non-equilibrium is produced by pumping the laser energy selectively into a particular vibrational level, and the resulting fluorescence monitored. By studying the time history of the fluorescence rise or decay from any particular level energy transfer rates involving that particular vibrational level can be obtained. This method, first used by Javan and coworkers[3], has proved to be extremely useful for obtaining molecular energy transfer rates for individual vibrational levels in contrast to the ultrasonic methods which give bulk relaxation times. This method has opened up the field for the study of the V-V energy transfer processes. The experimental methods and the results obtained are well reviewed[4]. However, selection of a suitable laser for studying excitation or deexcitation kinetics of a specific

vibrational level of a molecule is not always possible and practical difficulties limit the studies to temperatures below $\sim$ 1000°K .

The shock tube, on the other hand, is particularly suitable for studies at high temperatures. It has been a valuable research tool and had found applications in such diverse fields like aerodynamics, combustion and detonation processes, high temperature chemical kinetics, spectroscopy, astrophysics, molecular energy transfer studies etc. The shock tube is a device in which a plane shock wave is produced by the sudden bursting of a diaphragm which separates a gas at high pressure from one at lower pressure. The gas to be studied is filled in the low pressure section. At any given point in the low pressure side far from the diaphragm, the gas is rapidly brought to a high temperature, pressure and density by the passage of the shock wave. The region separating the initial and final equilibrium conditions is called the transition region. By measuring the time variation of an appropriate physical quantity during the transition period information regarding the physico-chemical processes taking place in that region can be obtained. For vibrational relaxation studies the two most important variables, measurements of which had yielded valuable data, are the density and infrared emission. The numerous experimental techniques and results of these measurements are summarised in references 5 and 6.

Kiefer and Lutz[7] developed the laser schlieren technique in 1966. In this method, the deflection of a narrow laser beam passing perpendicular to the shock tube axis is monitored while the shock wave is traversing it. This deflection is directly proportional to the density gradient in the transition region and provides information regarding the relaxation times. The laser schlieren method, which provides the most accurate and precise measurements of relaxation times, has since been used extensively[8-10]. This method has also been extended for the measurement of dissociation rates[11,12]. Recently, Bott[13] has developed an experimental technique which combines the shock tube and the laser induced fluorescence methods. This has the advantage of retaining the high temperatures of the shock tube and the selective excitation of the laser induced fluorescence method.

The aim of the present work is to study experimentally the molecular energy transfer processes in pure sulfur dioxide and sulfur dioxide-rare gas mixtures over a wide range of temperatures. SO_2 is one of the few molecules which exhibit a double relaxation behaviour. Lambert and Salter[14] made a careful study of SO_2 by ultrasonic methods and found that their results could be explained only if the vibrational excitation process occured as a double relaxation, a view which has been confirmed by later studies. Mccoubrey et al[15]

studied the effects of various additives like ethane, ethylene, water and n-hexane on the two relaxation times of SO_2. The rates of some of the V-V and V-T processes occuring in SO_2 and SO_2-Ar mixtures were obtained in the temperature range of 300-500°K from the careful ultrasonic studies by Shields[16] and Shields and Anderson[17]. The variation of relaxation times with temperature had also been studied upto 1100°K[18] in pure SO_2. Theoretical studies of SO_2 relaxation[19,20] confirm the presence of two relaxation regions and the calculated values of relaxation times are in fair agreement with experimental values at room temperature. Recently, the interest in sulfur dioxide relaxation studies has been revived by the thermal lensing[21] and laser induced fluorescence studies[22,23]. These studies suggest[22] that owing to the efficiency with which one vibrational manifold in SO_2 can be excited in preference to the other vibrational manifold, a significant population inversion between the stretching and bending modes can be achieved either by direct laser absorption or by indirect excitation transfer from another species.

Thus it may be useful to carry out a further study of vibrational relaxation processes in SO_2. The shock tube is ideally suited for measuring the relaxation times over a wide temperature range, from as low as 500°K upto the dissociation temperature. In view of the rapidity of the relaxation

processes in SO_2, the laser schlieren method of measuring the relaxation times is best suited for relaxation time measurements in SO_2. This technique enables one to make precise and accurate measurements of relaxation times that are as low as 0.5 μS.

In the present work relaxation times in SO_2, SO_2-Ar and SO_2-He mixtures are obtained over the temperature range 550°K - 2100°K using the shock tube - laser schlieren technique. The remainder of the thesis is organized as follows. Chapter II deals with the general theory of vibrational relaxation and discusses the interpretation of experimental data in terms of the various intra-molecular energy transfer rates. Chapter III is devoted to the presentation of the theory of laser schlieren technique and a description of the actual experimental set up used in this work. The results of the present investigation are presented and discussed in detail in Chapter IV. The present results are also compared with those of earlier workers in this chapter. The main conclusion of the present work are summarized in Chapter V.

CHAPTER - II

GENERAL THEORY OF VIBRATIONAL RELAXATION

II.1 INTRODUCTION

The process by which a sudden increase in the energy
of the molecules in a gas is distributed among the various
degrees of freedom of the molecules is very complex. This
process occurs through molecular collisions and if the gas
is not monoatomic the distribution of energy is not instan-
taneous. The translational degrees of freedom arrive at a
Maxwellian distribution within a few collisions. The rota-
tional degrees then equilibrate with translational degrees
fairly rapidly, the number of collisions for this process
being usually more than that required for translational
equilibration. However, the vibrational degrees take a much
longer time to equilibrate with the translational and the
rotational degrees of freedom. The time taken for the whole
vibrational energy to attain equilibrium may be represented
by a bulk or overall relaxation time, denoted by τ . It is
this time which is usually obtained in ultrasonic or shock
tube methods of studying vibrational relaxation in gases.

The rate at which the whole vibrational energy is
relaxing is related to the various rates at which energy
is being exchanged between the individual vibrational levels

of the gas molecules. The relation between the bulk relaxation time τ and molecular vibrational energy transfer rates for some simple cases is discussed below. This is followed by a discussion of the temperature dependence of the relaxation time.

II.2 RELAXATION IN DIATOMIC MOLECULES

In diatomic molecules, there is only one mode of vibration, and consequently, complexities arising out of intermode vibrational energy transfer are absent. In the following discussion, the diatomic molecule is approximated by a harmonic oscillator. This approximation is justified because the contribution of the higher energy levels to the observed relaxation rate is very small and hence the anharmonicity effects associated with the higher energy levels may be ignored.

The relaxation is characterized by a changing energy of vibration, E^{vib}. The differential equation describing the time variation E^{vib} is called the relaxation equation, which was derived by Landau and Teller[24] from general quantum considerations, with the assumption that the vibrational quantum number changes by only ± 1. If k_{10} and k_{01} are, respectively, the rates of de-excitation and excitation between the ground and first excited vibrational states, then it follows from

the principle of detailed balancing that

$$k_{01} = k_{10} \exp(-h\nu/kT) \tag{2.1}$$

where h = Planck's constant,

ν = frequency of the harmonic oscillator,

k = Boltzmann constant,

and T = translational temperature.

The rates for the other quantum states are given by

$$k_{n,n-1} = n\, k_{10} \tag{2.2}$$

and

$$k_{n-1,n} = k_{n,n-1} \exp(-h\nu/kT) \tag{2.3}$$

Then, if y_n is the number of molecules in the nth quantum state,

$$\frac{dy_n}{dt} = k_{n-1,n}\, y_{n-1} - k_{n,n-1}\, y_n + k_{n+1,n}\, y_{n+1} - k_{n,n+1} y_n \tag{2.4}$$

By multiplying the above equation by $nh\nu$ and summing over n, one can obtain the following expression for the rate of change of E^{vib} with time:

$$-\frac{\partial E^{vib}}{\partial t} = k_{10} \left[1-\exp(-h\nu/kT)\right]\ \left[E^{vib}-E^{vib}(T)\right] \tag{2.5}$$

where $E^{vib}(T)$ is the vibrational energy of the gas when it is in equilibrium with the translational temperature T. If the change in the translational temperature is negligible during the relaxation process, the solution of eq.(2.5) is given by

$$E^{vib}(T) = C \, \exp(-t/\tau) \tag{2.6}$$

where $\dfrac{1}{\tau} = k_{10} \, [\, 1-\exp(-h\nu/kT)\,]$ \hfill (2.7)

τ can be experimentally obtained by measuring the time variation of bulk quantities related to E^{vib}. From this, k_{10} can be calculated from eq.(2.7) and the other rates are obtained from (2.2) and (2.3). However, as already pointed out, anharmonic effects are important for the higher vibrational levels and the true rates for these levels are considerably larger than those given by (2.2) due to the reduced spacing between the higher energy levels.

II.3 RELAXATION IN POLYATOMIC MOLECULES

Relaxation in polyatomic molecules is complicated by the presence of intermode V-V energy transfer processes. Such a process can be described by

$$A(\lambda,a) + B\,(m,b) \longrightarrow A\,(\nu,a) + B(n,b) + \Delta E$$
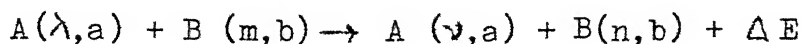
in which $A(\lambda,a)$ signifies a molecule A in the vibrational level λ of mode a. In the above process the molecule A in mode 'a' changes its quantum number from λ to ν, while the other molecule B in mode 'b' changes its quantum number from m to n upon collision. The difference in the vibrational energies of the colliding molecules goes into the translational and rotational degrees of the molecules. Then,

instead of a single relaxation equation like (2.5), the relaxation is described by a set of partial differential equations involving the transition probabilities for the above type of processes. Formulation of such equations and application to some real systems was given by Schwartz Slawsky and Herzfeld[26] and Tanczos[25]. A simplified treatment of relaxation in polyatomic molecules is given below.

Vibrational relaxation in a polyatomic molecule may occur by any of the following mechanisms: a) parallel b) series and c) series-parallel mechanism. These are discussed separately below:

a) Parallel mechanism: In the parallel mechanism, each vibrational mode equilibrates individually with the translational/rotational degrees of freedom. If each mode can be approximated by a harmonic oscillator, the equations derived in section (II.2) can be applied for each mode separately. Using eqs.(2.5) and (2.7), the parallel mechanism can be described by the following set of equations

$$- \frac{\partial E_s^{vib}}{\partial t} = \frac{1}{\tau_s} [\, E_s^{vib} - E_s^{vib}(T)]$$

(2.8)

where the subscript s refers to the individual vibrations. In this case the relaxation zone is characterized by as many relaxation times as the number of modes.

b) Series mechanism: The series process involves T/R-V activation of a single mode, usually the lowest energy mode, followed by the activation of the remaining modes by V-V energy transfer from this lowest energy mode. For illustration let us consider a molecule with only two modes, the lower of which is activated directly from translation with a relaxation time τ_1. The other mode exchanges energy with the first with a relaxation time τ_{23} . Then the relaxation can be described by the equations[2]

$$-\frac{\partial E_1^{vib}}{\partial t} = \frac{1}{\tau_1} [E_1^{vib} - E_1^{vib}(T_{tr})] - \frac{1}{\tau_{2,3}} [E_2^{vib} - E_2^{vib}$$

$$-\frac{\partial E_2^{vib}}{\partial t} = \frac{1}{\tau_{2,3}} [E_2^{vib} - E_2^{vib}(T_1^{vib})]$$

where E_1^{vib} and E_2^{vib} are the vibrational energies of mode 1 and mode 2 respectively at any time t,

$E_1^{vib}(T_{tr})$ = vibrational energy of mode 1 in equilibrium at the translational temperature

and $E_2^{vib}(T_1^{vib})$= vibrational energy of mode 2 in equilibrium at the instantaneous vibrational temperature of mode 1.

Usually, the intramolecular V-V rates are quite large compared to the V-T/R rates, so that $\tau_{2,3} \ll \tau_1$. For such a

case, it had been shown[2] that the entire relaxation zone can
be characterized by a single relaxation time τ given by

$$\tau = \tau_1 \frac{C_1{}^{vib} + C_2{}^{vib}}{C_1{}^{vib}} \qquad (2.10)$$

where $C_1{}^{vib}$ and $C_2{}^{vib}$ are the vibrational specific heats of
the modes 1 and 2, respectively. This result can be extended
to the case where n vibrational modes are involved and where
all the inter-mode energy transfer rates are fast compared
to the T/R-V rate of the lowest mode. Then eq.(2.10) becomes

$$\tau = \tau_1 \frac{C_1{}^{vib} + C_2{}^{vib} + ...+ C_n{}^{vib}}{C_1{}^{vib}} \qquad (2.11)$$

and the relaxation equation is given by

$$-\frac{\partial E^{vib}}{\partial t} = \frac{1}{\tau} [\, E^{vib} - E^{vib}(T_{tr})\,]$$

Here E^{vib} is the total instantaneous vibrational energy,

$$E^{vib} = E_1{}^{vib} + E_2{}^{vib} + ...+ E_n{}^{vib}$$

On the other hand, if the intramolecular V-V rate
is smaller than or comparable to the V-T/R rate at which
the lowest mode is relaxing, then the relaxation process
involves more than one relaxation time.

c) Series – parallel process: In a combination series-
parallel mechanism, the V-T/R energy transfer involves more

than one vibrational mode, the rest of the vibrational modes being excited by V-V energy transfer processes. This mechanism is not generally considered.

II.4 TEMPERATURE DEPENDENCE OF RELAXATION TIMES

Landau and Teller were the first to derive an expression for the temperature dependence of the probability of energy transfer during a collision by a purely classical treatment. According to them the effectiveness of a given collision in exciting or de-exciting a periodic degree of freedom depends on the degree to which the collision can be considered as adiabatic. A collision is assumed to be strictly adiabatic if the degree of freedom under consideration undergoes an infinite number of cycles during the time of contact. In such a case, there is zero probability that the mode will change its state during the collision. However, if the collision is not adiabatic, i.e. if there are only a finite number of oscillations during the perturbing effect of the collision, then energy may be transferred from translation to the degrees of freedom under consideration. This was expressed mathematically by using the ratio

$$X = t_c/t_0$$

where t_c is the duration of collision and t_0 is the natural

period of the degree of freedom. If χ is of the order of unity or less, then only a few collisions are necessary to bring the degree of freedom into equilibrium, while many collisions will be needed for equilibration when χ is larger than unity. In the case of vibrational degree of freedom, t_c and t_0 can be written as

$$t_c = r/\overline{v}' \quad \text{and} \quad t_0 = \frac{1}{2\pi\nu}$$

where r is the "range" of molecular interaction, $\overline{v}'$ is the relative velocity of the two colliding molecules and ν is the frequency of vibration.

Then $\quad \chi = \dfrac{2\pi\nu r}{\overline{v}'}$ $\hspace{2cm}$ (2.12)

when $\chi \gg 1$, as is the case for vibration, Landau and Teller showed that P_{10}, the probability per collision of de-exciting a molecule in the first excited state, is given by

$$P_{10} = C \exp(-\chi) \hspace{2cm} (2.13)$$

where C is a factor that depends on the geometry of collision. Eq.(2.13) must be generalized to include all of the molecules in the gas by averaging over the Maxwellian velocity distribution. When this is done, the following expression is obtained

$$P_{10} = K_1 T^{-1/3} \left[\exp(-K_2/T^{1/3})\right] \quad (2.14)$$

K_1 and K_2 are constants which depend on collision cross-sections. Now, P_{10} is related to k_{10} by the equation

$$N \, P_{10} = k_{10} \qquad (2.15)$$

where N is the number of collisions per unit time. Therefore, eq.(2.7) can be written as

$$\frac{1}{\tau} = N \, P_{10} \, [1-\exp(-h\nu/kT)] \qquad (2.16)$$

or since $N \propto PT^{-1/2}$, where P is the pressure,

$$\tau = \frac{K_1' \, T^{1/6} \, \exp(K_2/T^{1/3})}{P \, [1-\exp(-h\nu/kT)]} \qquad (2.17)$$

This expression shows immediately that $\tau \propto 1/P$, or $P\tau$ is a constant for a given temperature. As a first approximation, the term $[1-\exp(-h\nu/kT)]$ can be put equal to 1, and as $T^{1/6}$ is a weak function of T , eq.(2.17) shows that

$$P\tau \propto \exp(K_2/T^{1/3})$$

$$\text{or} \quad \log(P\tau) \propto T^{-1/3} \qquad (2.18)$$

This result is widely used for the interpretation of experimental results by many workers. Later, Schwartz, Slawsky and Herzfeld (SSH) derived the same result[26] with

an approximate three-dimensional quantum mechanical treatment. They found that

$$P_{10} \sim \exp\left[-3(\Delta E^2 \, \mu\pi^2/2 \, \alpha^2 \, \hbar^2 \, kT)\right]^{1/3} \qquad (2.19)$$

where ΔE = amount of energy exchanged with translation,

μ = reduced mass,

α = relative approach velocity,

and k = Boltzmann constant.

Substituting this expression for P_{10} in eq.(2.16), it can be easily seen that the same temperature dependence as given by eq.(2.18) is obtained.

In most of the vibrational energy transfer processes where large amounts of energy are exchanged with translation, the temperature dependence and the magnitude of the energy transfer probabilities by the SSH theory are consistent with the available experimental data in many systems[6].

For V-V energy transfer processes in which the energy exchanged with translation is small the temperature dependence is generally quite different from that given by eq.(2.19). A general discussion of such processes, called near resonant V-V energy transfer processes, is discussed elsewhere[4].

CHAPTER - III

EXPERIMENTAL

III.1 THE LASER SCHLIEREN TECHNIQUE

The change in density across the shock wave during vibrational relaxation had been an extremely useful quantity in estimating the vibrational relaxation times. The fact that the refractive index of a gas is directly proportional to the density is the basis of all densitometric measurements in shock heated gases. A light beam passing across the shock tube is deflected progressively towards the higher density side as the density and hence the refractive index change during relaxation. The light beam coming out of the shock tube is focussed on to a knife edge which is initially adjusted such that it prevents, totally or partially, the light beam from falling on a photomultiplier behind it. The progressive deflection of the light beam, caused by relaxation of the gases in the shock tube, causes the focussed image to shift in space, and the knife edge allows more and more light to escape and fall on the photomultiplier. The voltage change recorded by the photomultiplier is thus a measure of the deflection of the light beam and hence of the density behind the shock wave. Resler and Scheibe[27] developed an integrated schlieren technique using a light source - knife

edge - photomultiplier combination to study the relaxation
zone in a shock wave. Kiefer and Lutz[28] developed a very
sensitive quantitative schlieren method in which a knife edge-
photomultiplier detection of a narrow laser beam is used to
obtain a close approximation to a point measure of the density
gradient. This method is similar to that of Resler and Scheibe
but differs in its use of a laser beam. The high sensitivity
of the laser schlieren technique is a consequence of the
extreme brightness and narrow beam diameter of the laser. The
narrow beam of the laser is advantageous since it avoids the
problem of non-linear response of schlieren systems with
highly parallel light without significant loss of sensitivity.
In the laser schlieren technique, the laser beam from a He-Ne
laser passes through the shock tube perpendicular to the tube
axis, travels a distance of a few meters and falls on a knife
edge. The knife edge is initially adjusted so that it cuts the
cross-section of the beam vertically into two equal halves.
In this position, one half of the beam is blocked by the knife
edge and the other half is allowed to fall on to a photo-
sensitive device placed behind the knife edge. As the shock
wave traverses the observation station, the beam gets deflec-
ted from its initial position at the knife edge and the
photosensitive device receives more or less light depending
on the position of the knife edge. This change in light

intensity is converted into a suitable voltage change and recorded on an oscilloscope. Such oscilloscope traces are characterized by an initial 'spike' when the shock front arrives at the observation station, followed by a slower change due to the subsequent vibrational relaxation in the shock wave.

The various aspects of the laser schlieren technique are discussed in Ref.7. A brief review is given below. The beam from a uniphase gas laser has a nearly Gaussian power distribution across its wave front, i.e., if the z-axis is taken to be the direction of propagation, then the power distribution in the x,y plane is given by

$$P\ (x,y) = \left(\frac{P_0}{\pi\sigma^2}\right)\ \exp\ [\ -(x^2+y^2)/\sigma^2]\ \ \ \ \ \ \ \ \ (3.1)$$

where P_0 is the total beam power and σ is the standard deviation of the Gaussian function ($\leftrightarrow$ beam diameter). If the photodetector responds linearly to the light intensity and if the beam is initially centered at the knife edge, then for a deflection D from this position, the corresponding voltage change can be obtained by integrating eq.(3.1) between the appropriate limits. This is given by

$$\left|\frac{\Delta V}{V_0}\right|\ = \tfrac{1}{2}\ erf\ (D/\ \sigma_x\ )\ \ \ \ \ \ \ \ \ (3.2)$$

where V_0 is the voltage output when the whole beam falls on the photodetector and σ_k is the standard deviation of the Gaussian distribution (3.1) at the knife edge. If D is small compared to σ_k , eq.(3.2) can be written as

$$\left| \frac{\Delta V}{V_0} \right| = \frac{D}{\sqrt{\pi} \, \sigma_k} \left[1 - \frac{D^2}{3 \, \sigma_k^2} + \ldots \ldots \right] \qquad (3.3)$$

If $|\Delta V/V_0| \leqslant 0.15$, then the non-linear term in (3.3) is less than 2.2×10^{-2}, and hence the voltage output is linear with D to about 2%. So, for small deflections, (3.3) becomes

$$\left| \frac{\Delta V}{V_0} \right| = \frac{D}{\sqrt{\pi} \, \sigma_k} \qquad (3.4)$$

Now, the deflection D is related to the local density gradient in the shock wave by the equation

$$D = RLW \frac{d\rho}{dx} \qquad (3.5)$$

where R = specific refractivity of the test gas,

L = distance travelled by the laser beam from the centre of the shock tube to the knife edge,

W = internal diameter of the shock tube,

and $d\rho/dx$ = local density gradient in the shock wave.

Combining eqs. (3.4) and (3.5), we get

$$\left|\frac{\Delta V}{V_0}\right| = \frac{RLW}{\sqrt{\pi}\ \sigma_k}\ \frac{d\rho}{dx} \qquad (3.6)$$

This equation is valid only for the relaxation zone. The voltage change corresponding to the initial 'spike' of the schlieren signals is due to a large density gradient across the shock front. This large density gradient is the result of rapid equilibration of translational and rotational energy of the shocked gas. If ε is the thickness of the shock front, then it can be shown that

$$\left|\frac{\Delta V}{V_0}\right|_{max} = \tfrac{1}{2}\ \text{erf}\ (\varepsilon/2\ \sigma_t) \qquad (3.7)$$

where $\left|\dfrac{\Delta V}{V_0}\right|_{max}$ = voltage corresponding to the peak of the initial 'spike',

and σ_t = standard deviation of the Gaussian function (3.1) inside the shock tube.

The time taken for the shock front to effectively leave the beam before quantitative gradient measurements can be made is indicative of the possible spatial resolution of the laser schlieren technique. This time is dependent on ε and is generally below 0.5 μS .

Measurement of relaxation times

For a gas in which the vibrational relaxation can be described by the equation

$$-\frac{\partial E^{vib}}{\partial t} = \frac{1}{\tau} \, [E^{vib} - E^{vib}(T)] \; ,$$

Blackman[29] had shown that the density variation can be given by

$$\frac{\rho - \rho_2}{\rho_a - \rho_2} = \frac{\rho_2}{\rho_a} \exp \, (-C_p t / C_p' \tau) \qquad (3.8)$$

where ρ = density of the relaxing gas,

      ρ_a = density in the region immediately behind the shock where translational and rotational energy are equilibrated, with no change in the vibrational energy,

      ρ_2 = density in the final equilibrium state,

      C_p = specific heat at constant pressure of the relaxing gas,

and C_p' = specific heat due to translation and rotation only.

Differentiating eq.(3.8) with respect to time, we get

$$\frac{1}{(\rho_a - \rho_2)} \cdot \frac{d\rho}{dt} = \frac{\rho_2}{\rho_a} \cdot \exp \, (- C_p t / C_p' \tau) \cdot (- \frac{C_p}{C_p' \tau})$$

$$\text{or} \; \frac{d\rho}{dt} \propto \exp \, (- C_p t / C_p' \tau) \qquad (3.9)$$

Since $\dfrac{d\rho}{dx} = \dfrac{d\rho}{dt} \cdot \dfrac{dt}{dx} = \dfrac{1}{u_s} \cdot \dfrac{d\rho}{dt}$ where u_s = shock velocity,

eq.(3.9) can be written as

$$\frac{d\rho}{dx} \propto \exp\left(- C_p t / C_p' \tau \right) \qquad (3.10)$$

substituting in eq.(3.6), we get

$$\left|\frac{\Delta V}{V_O}\right| \propto \exp\left(-C_p t / C_p' \tau \right) \qquad (3.11)$$

Eq.(3.11) shows that a plot of log ΔV against time should yield a straight line with slope $(C_p/C_p'\tau)$. Let the inverse of this slope be called τ_L, the laboratory relaxation time. Then,

$$\tau = \tau_L \cdot \frac{C_p}{C_p'} \quad .$$

After converting laboratory times to particle times and normalizing to one atmosphere, the relaxation time at one atm., $(P\tau)$, is given by

$$(P\tau) = \tau_L \cdot \frac{C_p}{C_p'} \cdot \frac{\rho}{\rho_1} \quad . P \qquad (3.12)$$

where ρ_1 is the density of the unshocked gas. Several workers had taken the values of C_p', ρ and P as the average values between the just-after-shock front and the final equilibrium states. The temperature corresponding to $(P\tau)$ was also averaged in a similar way. The values of $(P\tau)$ obtained in this way are sometimes called Blackman times.

It had been pointed out[30] that the Blackman times some what overestimate the true values. This is due to the assumption made in deriving eq.(3.8) that the relaxation proceeds under conditions of constant translational temperature. Other methods[9,31] are available for evaluating relaxation times at any point in the relaxation zone. These methods take into consideration the changing translational temperature in the relaxation zone. In what is called the modified Blackman method, the values of C_p, ρ, P and T used in eq.(3.12) are taken at the final equilibrium conditions. These values differ by about 4% from the actual values[32].

III.2 EXPERIMENTAL SET UP

A diagrammatic sketch of the experimental set up is shown in fig.(3.1).

The shock tube

A complete description of the conventional and operational details of the shock tube was given in an earlier thesis[33]. Briefly, the shock tube consists of a high pressure driver section and a low pressure driver section. The driver section is a 1.68 m. long stainless steel cylindrical tube of 15.3 cm. internal diameter. The low pressure section is a 5.72 m. long honed stainless steel cylindrical tube of 9.85 cm.

To pump

M

W

W

He–Ne laser

Amp

TFG1 TFG2

Amp

To manometer

SO

C

To pump &
gas handling

D

P.D. Lens K.E.

Pressure gauge

Driver gases

To pump
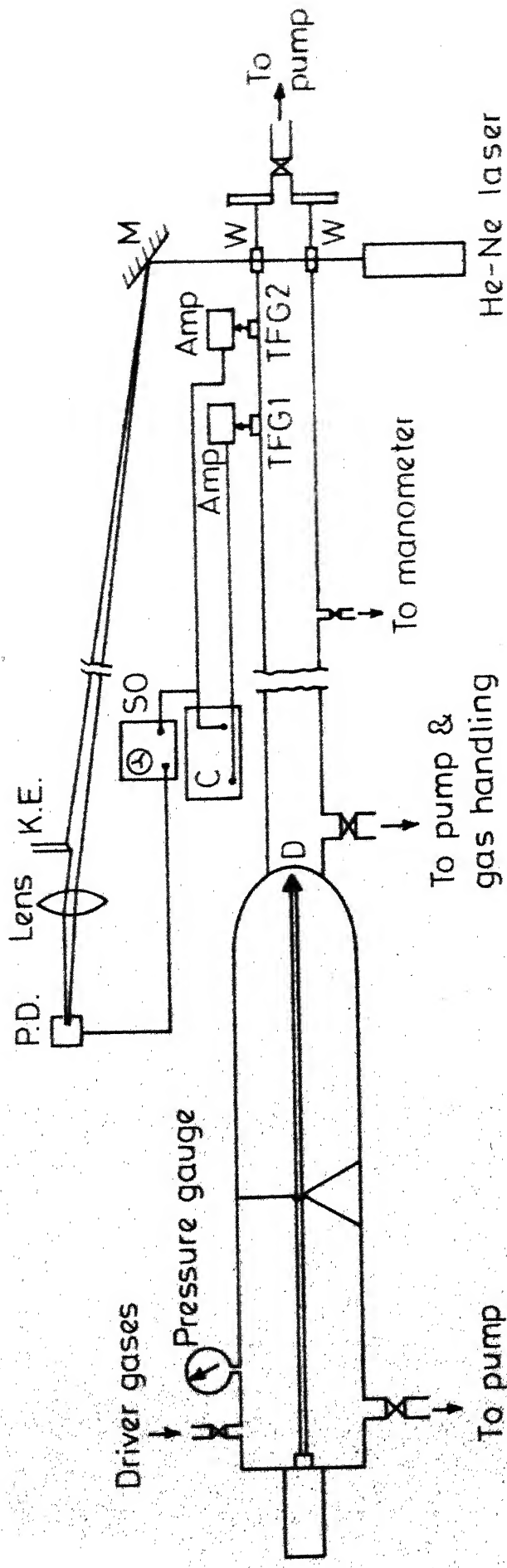
W – Glass window

C – Counter

KE – Knife edge

PD – Photo diode assembly

D – Diaphragm

diagram of shock tube.

internal diameter. The high pressure and low pressure sections
are joined by an intermediate section whose diameter varies
continuously from 15.3 cm. to 9.85 cm. This intermediate
section is permanently attached to the high pressure section.
The high pressure and low pressure sections can be locked
together or dismantled by means of the coupling device shown
in fig.(3.2). The whole shock tube is mounted on wheeled iron
stands which are in turn mounted on iron rails.

Shock waves are generated by bursting mylar sheets
of 0.005" thickness by a pnuematically operated mechanical
plunger. The plunger runs along the axis of the driver section
and is supported by stands as shown in fig.(3.1). Mixtures of
H_2, N_2, He and CO_2 are used in the high pressure sections to
obtain the required variations in the shock velocities. The
driver section can be evacuated to an ultimate vacuum of
2×10^{-5} torr with the help of a vacuum system consisting
of a 4" silicone oil diffusion pump backed by a roughing pump.
The driver section is evacuated by a separate mechanical
pump. The combined leak and degassing rate in the driver
section was measured intermittently, and was always found to
be less than 5×10^{-4} torr/minute.

Measurement of shock speed

The shock speed was measured by means of two gold
resistance gauges mounted flush with the walls of the
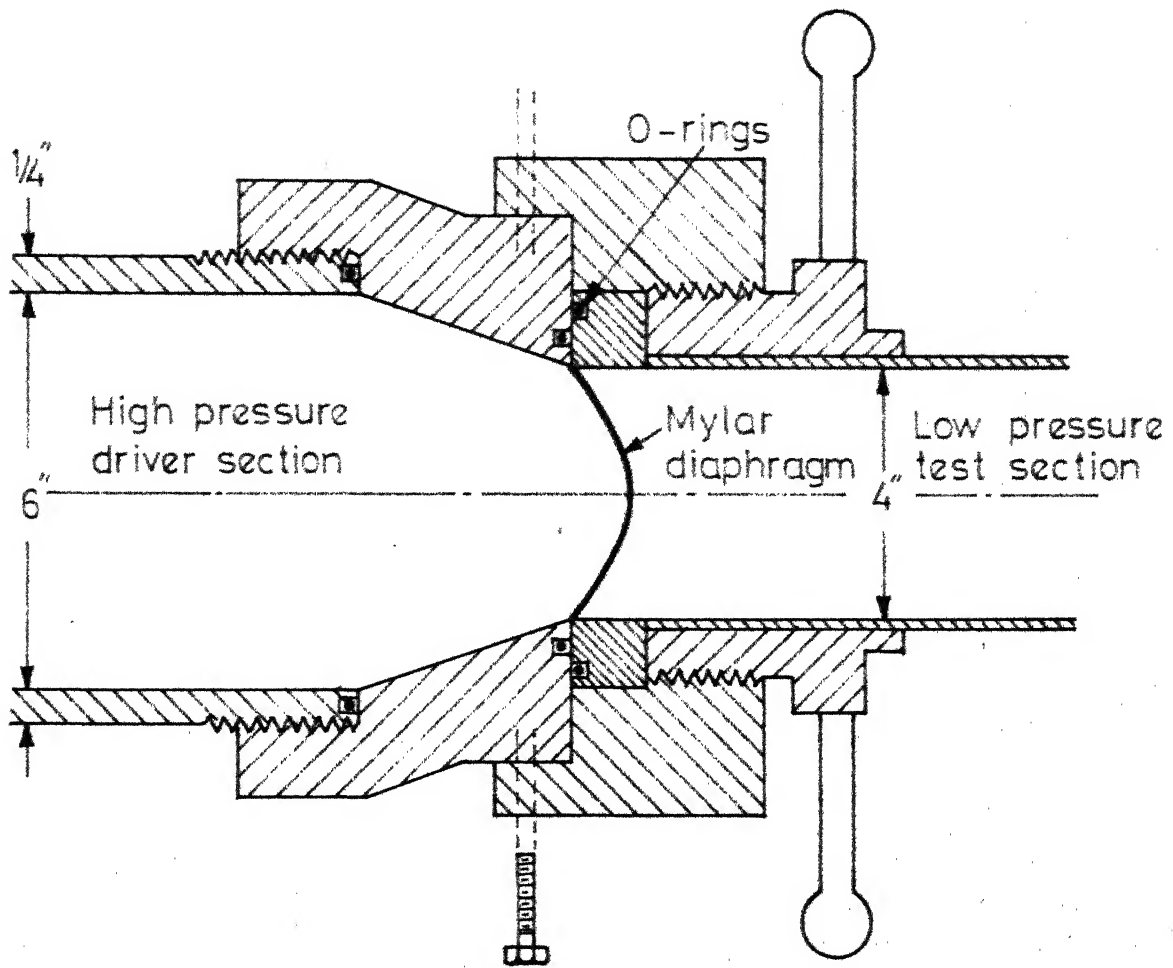
Fig.3·2(a)-Diaphragm Clamping Arrangement.
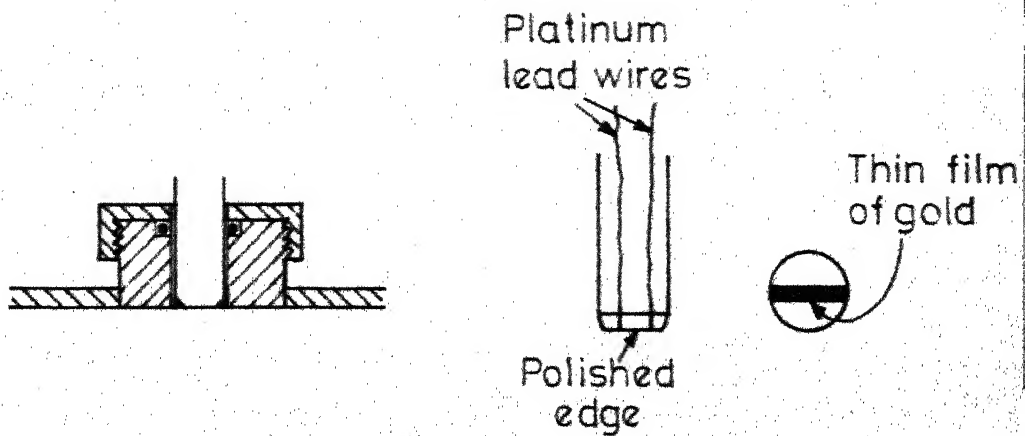
Mounting for thin film gauge.　　Thin film gauge.

shock tube. As the shock wave attenuation is small, only two resistance gauges are used to obtain the shock velocity[34]. The thin film gauges are prepared by vacuum deposition of gold on to platinum-glass tubes closed at one end. The glass tubes of $\frac{1}{2}$" diameter are sealed at one end after inserting two platinum wires. After polishing this end sufficiently, the cross-sections of the platinum wires appear as small circles on the closed end. Gold is now evaporated on to this end to form a thin film of about 1 mm. width, thus making electrical contact between the film and the platinum leads. The resistance of the film is continuously monitored during vacuum deposition, and the evaporation of gold is stopped when the resistane of the film is about $50\,\Omega$. These thin film gauges are then mounted on the shock tube with the longer dimension of the film perpendicular to the shock tube axis. The thin film gauge and the mounting is shown in fig.(3.2b). The first of these two is at a distance of 4.25 m. from the diaphragm station and the second is placed 78.5 cm away from the first one. The windows for passing the laser beam are placed 5 cm. after the second thin film gauge. As the shock front passes across the thin film gauges, the change in the resistance of the thin films is converted into voltage signals, which, after suitable amplification, are used to start and stop a Beckman model 7370 digital counter. The

distance between the thin film gauges, divided by the time obtained in the counter is equal to the shock speed at the observation station. The rise time of the thin film gauge is found to be roughly equal to the transit time of the shock front across it, which is about 1 μS.

The pressure in the driven section is measured by means of a silicone oil manometer. The pressure in the driver section is measured directly by a Bourdan pressure gauge.

Gases

A GLC analysis of the SO_2 gas used showed the presence of about 2% of combined O_2 and N_2 as impurities. To evaluate the effect of these impurities on the measured relaxation times, SO_2 was frozen at liquid nitrogen temperature and the residual gases pumped out for about 15 minutes. It was then melted and a fraction of the evaporating gas was pumped out. The middle fraction was directly taken into the shock tube. The relaxation times obtained for purified SO_2 and those for SO_2 taken directly from the cylinder did not show any marked difference as can be seen from fig.(4.4). The black circles in fig.(4.4) correspond to purified SO_2 and the open circles to SO_2 directly taken from the cylinder. Hence all the experiments are conducted with the SO_2 taken directly from the cylinder. High purity Matheson Helium (99.995%) and ultra high

purity Argon (99.999%) from Indian Oxygen Ltd. were used.
High purity bonedry Matheson CO_2 (99.99% pure) is used for
preliminary test runs.

Mixtures of SO_2-He and SO_2-Ar were prepared in a stain-
less steel mixing chamber. The mixing chamber is evacuated with
a diffusion pump for about 24 hrs. and the gases are filled in
the appropriate proportion to a total pressure of about
50 psia. The partial pressures are read by a Bourdan pressure
gauge. Gases are allowed to pass into the mixing tank slowly
until a preset mark in the pressure gauge is reached. This is
done to minimize the errors in concentration measurement. The
gases, after filling in the mixing tank to the desired pressures,
are left for more than 24 hrs. before use to ensure thorough
mixing.

Laser schlieren system

The observation station, i.e., the point where the laser
beam passes through the shock tube is located 5 cm. down stream
of the second thin film gauge and 3.5 cm before the end plate.
The reflected shock wave did not cause any interference since
the relaxation processes are over usually within 10 μS ,
whereas the reflected shock would arrive only after 50-100μS.
Glass windows of 1" diameter, fixed in plexi-glass adoptors

are mounted flush with the wall. These windows are cleaned frequently to ensure the gaussian distribution in the laser beam.

The 6329 Å laser beam from a 0.5 mw spectra Physics model 156 He-Ne laser was passed through the shock tube through these windows perpendicular to the shock tube axis. It is important that the beam should be perpendicular to the tube axis. Otherwise, the spatial resolution will be decreased. The laser is adjusted perpendicular to the tube axis by means of two rectangular blocks. Repeated runs in Argon, with the laser removed and adjusted again did not show any difference in the resolution, showing that the perpendicularity is good. The laser beam coming out of the tube is reflected by an aluminum coated mirror to fall on a knife edge. The distance from the shock tube centre to the reflecting mirror is 1.35 m. and the distance from the reflecting mirror to the knife edge is 5.49 m. The light that was not cut off by the knife edge was collected by a 7 cm. diameter lens and focussed on to a HP type 5082-4203 pin photodiode. The pin-photodiode with the associated amplifier is mounted on a device which can be moved in the x,y,z directions so that the pin-photo-diode could be adjusted very precisely to receive all the light collected by the lens. The knife edge can be moved smoothly

so that it can be adjusted to cut the laser beam along the
vertical diameter. The pin-photodiode assembly, the glass
lens and the knife edge are mounted on an iron bench. The
laser and the reflecting mirrors are mounted on separate
iron benches. The reflecting mirror can be rotated at a
uniform speed so that the laser beam can sweep across the
knife edge at a uniform rate. The resulting output from the
photodiode is then the integrated Gaussian given by eq.(3.2)
and can be used to test the linearity of the detection system.
As the beam is sweeping past the knife edge at constant speed,
D in eq.(3.2) is a linear function of time. The voltage output
from the photodiode as the beam sweeps across it is given in
fig.(3.3). It can be seen that this curve is linear in the
central portion. The linear portion of this calibration
extends to approximately $\pm$ 20% from the centre. Thus it is
ensured that the photodiode output in the central portion of
the beam varies linearly with the deflection of the beam and
hence with the local density gradient in the shock wave.

The photodiode responds linearly for six decades of
light intensity and hence the problems of saturation, which
are common with a phtomultiplier are eliminated. The dark
current noise encountered in photomultipliers is also
absent. It is easy to handle because no high voltagesiere
involved.
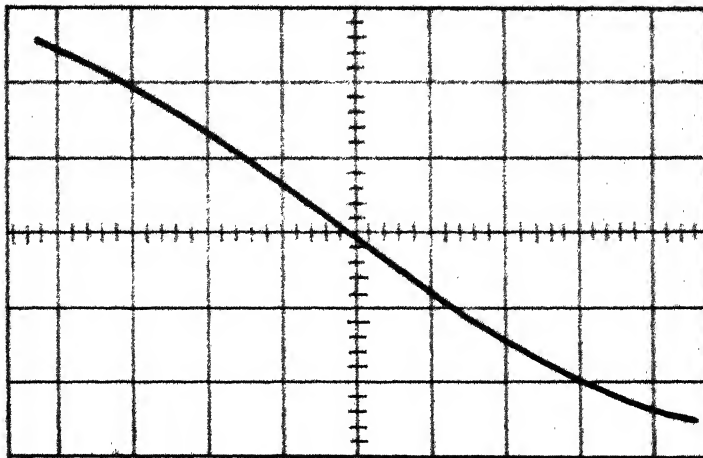
Fig. 3·3 – Photo diode output as the laser beam
sweeps across the knife edge.

Vert. scale : 10 mV/cm

Horz. scale : 0·5 µS/cm

Speed of the motor : 980 rpm

The photodiode output, suitably amplified, is fed directly to a Tek type 1A5 plug-in amplifier fitted into a Tek type 549 storage oscilloscope. The oscilloscope is operated in a single sweep mode and triggered with the signal from the thin film gauge just ahead of the observation station.

The overall response time of the system is measured by firing shocks into Argon. Fig.(3.4) shows a typical schlieren record obtained in Argon. It is found that the schlieren record decays with a time constant of $0.12\mu S$ which may be taken as the time constant of the detection system. At high shock velocities and low pressures in the test section, there is a possibility that this time may be more due to shock wave curvature. Taking these points into consideration, the schlieren records which showed time constants of less than $0.35\mu S$ have not been included in the analysis.

Procedure

After locking the driver and driver section with a mylar diaphraghm in between, the driver section is evacuated to about 5 microns with the help of two roughing pumps. After this, the diffusion pump is switched on and the pressure
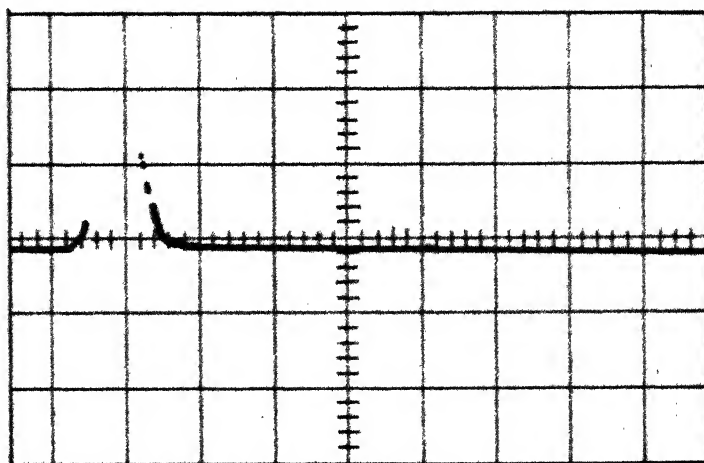
Fig.3.4(a)– Laser schlieren record in Argon.
Vert. scale : 50 mV/cm
Horiz. scale: 1 μS/cm
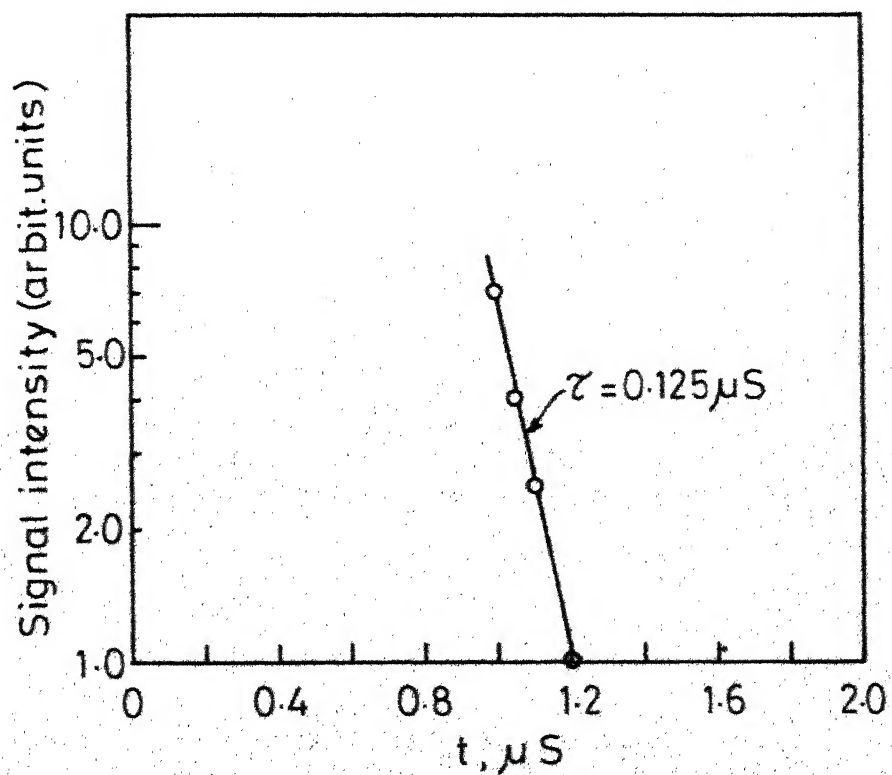
Fig.3.4(b)– Semi-log plot of fig. 3.4(a).

brought down to about 5×10^{-5} torr. Evacuation is continued for about 2 hrs. Runs taken with evacuation times varying from 2 to 10 hrs. did not show any difference and hence the minimum of 2 hrs. is usually taken. The driver section is also evacuated by a roughing pump. After this, the driver section was filled with gases of the required composition and pressure. The knife edge is moved away from the lens and a chopper is placed in the path of the laser beams This produces an a.c. signal from the photodiode with its peak corresponding to the whole beam falling on to the photodiode. Let this peak voltage be V_0. Now the knife edge is brought slowly so as to cut the light falling on the photodiode, until the peak voltage is equal to $\frac{1}{2} V_0$. The beam is now centered and the chopper removed from the path of the beam. The test gas is now filled into the driver section to the desired pressure and the shock is fired by releasing the mechanical plunger. The counter time is noted for shock-speed calculations, and the schlieren record stored on the oscilloscope is photographed with a polaroid camera. The voltages at the various time intervals are read by keeping a transparent graph sheet on the photograph. The relaxation times are finally obtained by measuring the slopes of the lines resulting from the semi-log plots of voltage vs time.

The equilibrium values of temperature, pressure, density etc. are calculated by solving the mass, momentum and energy conservation relations by an iterative procedure on a computer. The input to the computer consists of the shock velocity, the conservation relations, the ideal gas law, and the enthalpy – temperature equation. The enthalpy data is taken from NASA special report SP-3001.

CHAPTER - IV

RESULTS AND DISCUSSION

IV.1 RELAXATION TIME MEASUREMENTS IN CO_2

Vibrational relaxation times in pure carbon dioxide
are measured with the present set-up in the temperature region
600°K - 1600°K. This is done with the objective of checking
the whole system by comparing the results obtained with this
set-up with the measurements reported earlier by other workers.
A typical schlieren signal in CO_2 and its semi-log plot are
shown in fig.(4.1). As in all laser schlieren studies, the
signal shows a sharp spike as the shock front arrives at the
observation station. This spike whose peak goes off the scale
on the scope, is followed by a slow decrease in the signal.
As can be seen from fig.(4.1), the signal exhibits a single
exponential behaviour throughout the relaxation region without
any observable deviation. The slopes obtained from such plots
are used to obtain the relaxation times by using the modified
Blackman expression as discussed in the previous chapter. The
results are tabulated in Table(4.1). Simpson and Chandler[9]
made thorough and accurate measurements of relaxation times
in CO_2 using the laser schlieren technique. Their results,
shown by the solid line, are plotted along with those obtained
in the present study in fig.(4.2). It can be seen from this
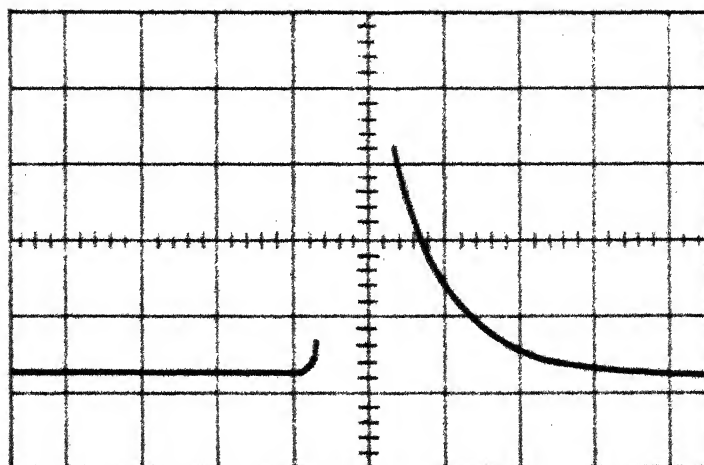
Fig.4.1(a)- Laser schlieren signal in pure CO_2.
Time scale: $2\,\mu S/cm$
$p_1 = 2\cdot24$ torr, $T_2 = 992\cdot4°K$
$u_S = 1\cdot229\,mm/\mu S$

$\tau_L = 1.433\,\mu S$
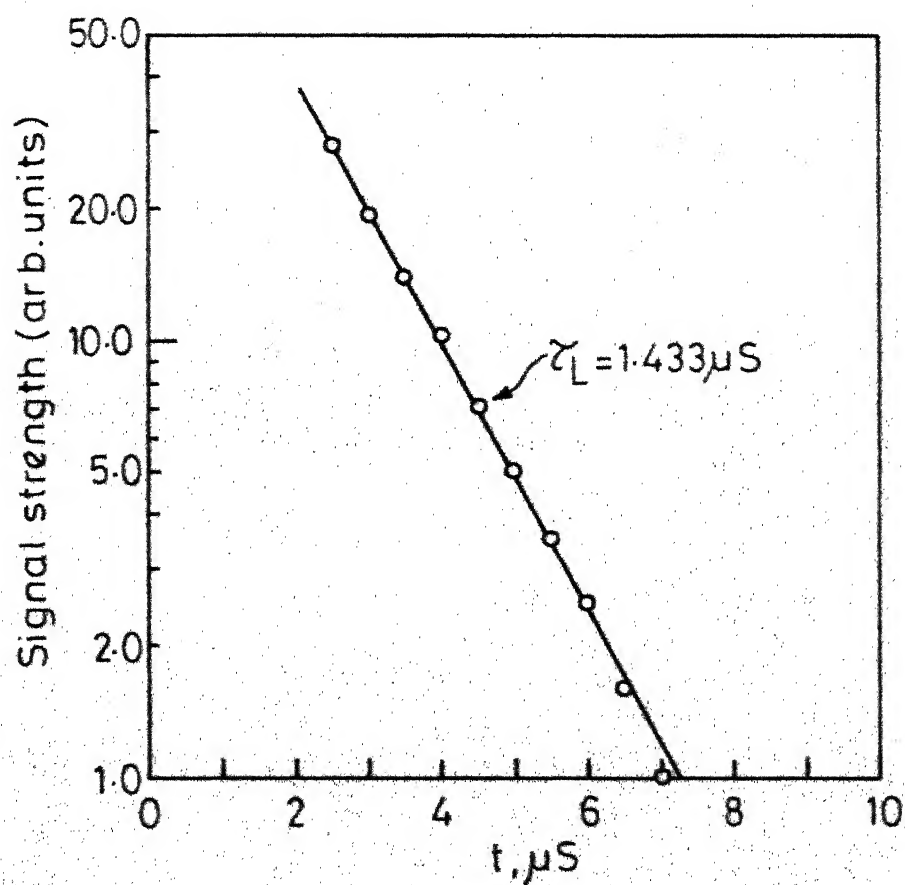
Table No. 4.1

Vibrational relaxation data in CO_2

S.No.	p_1 (mmHg)	u_s (mm/μS)	T_2 (°K)	τ_L (μS)	$P\tau$ (atm.μS)
1	1.36	1.732	1578.0	0.652	1.038
2	2.40	1.156	921.5	2.140	1.790
3	2.24	1.229	992.4	1.390	1.395
4	2.40	1.407	1183.0	0.783	1.200
5	2.16	1.596	1397.4	0.548	1.092
6	2.32	1.406	1183.0	0.938	1.404
7	2.40	1.351	1118.0	0.913	1.236
8	2.44	1.086	855.6	2.440	1.704
9	2.44	1.023	796.5	3.130	1.805
10	2.40	0.954	738.9	4.500	2.028
11	2.32	0.865	664.3	5.440	2.514
12	4.16	0.820	631.2	7.020	3.312
13	4.64	0.746	575.8	7.350	2.760
14	5.68	0.796	612.9	5.000	2.892
15	5.28	0.752	581.6	6.980	3.078
16	6.56	0.776	600.0	5.350	3.480
17	7.48	0.748	577.8	4.520	2.990
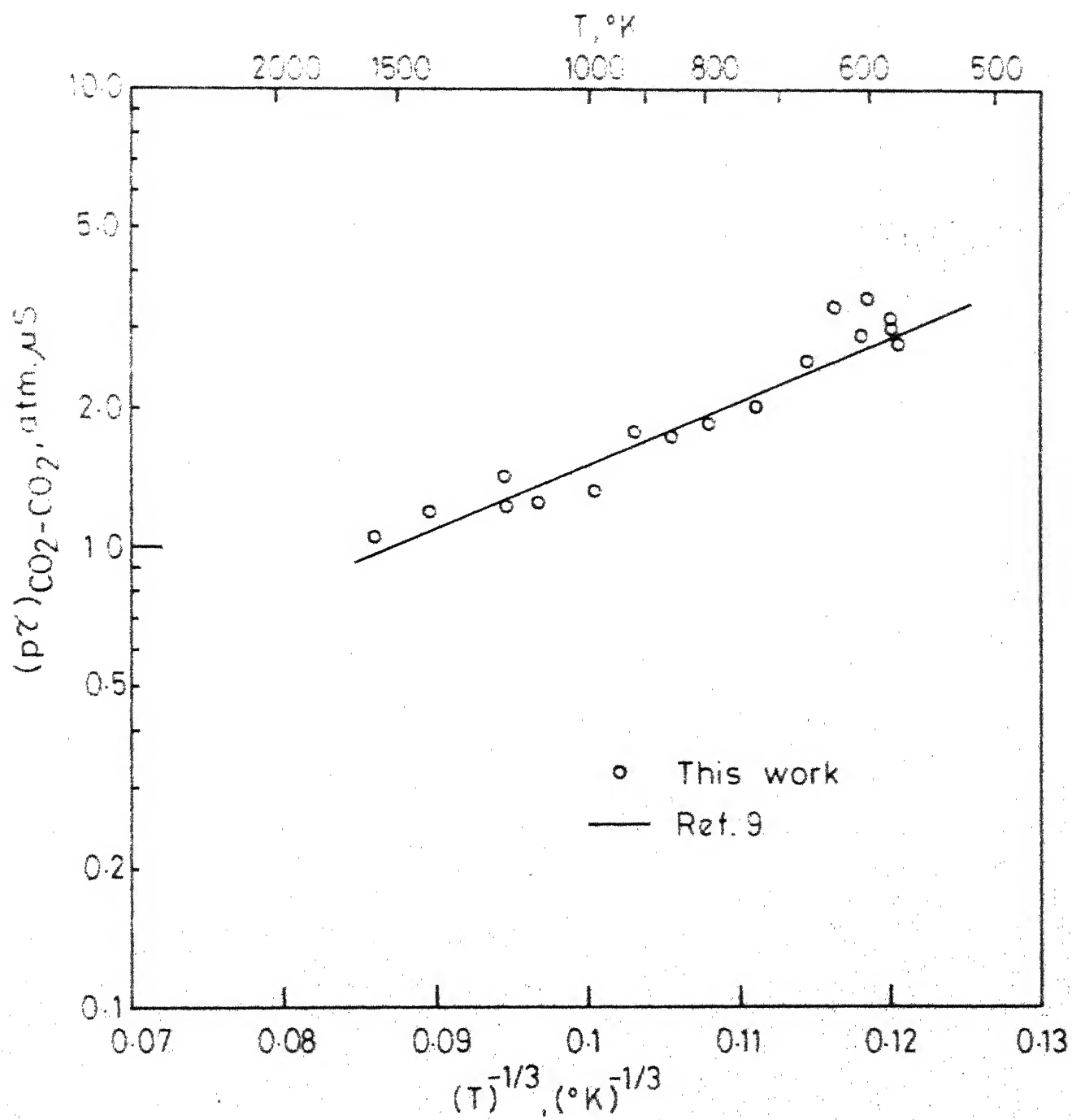
Fig. 4·2 – Vib. relaxation times in pure CO_2.

fig. that the present results are in very good agreement with
those of Simpson and Chandler.

IV.2 RELAXATION MEASUREMENTS IN PURE SO_2

Density gradient profiles in incident shocks are
obtained in pure SO_2 in the temperature range of 550°K - 1200°K.
Measurements could not be extended beyond 1200°K owing to
limitations imposed by the photodiode response time. In
making measurements on moving gases, the times measured in
the laboratory are reduced by a factor of (ρ_2/ρ_1) where ρ_2
and ρ_1 are the post-shock and pre-shock densities[5]. Since
(ρ_2/ρ_1) is as much as 10 for temperatures above 1000°K for
SO_2, the effective resolution of the detecting device is
reduced by a factor of 10. This limits us to measurements
below 1200°K.

A typical oscilloscope trace of the laser schlieren
signal in pure SO_2 and its semi-log plot are given in fig.(4.3).
It can be seen that the first few points clearly deviate
from the straight line plots . This behaviour is absent in
CO_2. But in SO_2, more than 30% of the schlieren records show
this behaviour. This behaviour is observed in mixtures of
SO_2-Ar and SO_2-He also and is discussed in later sections.
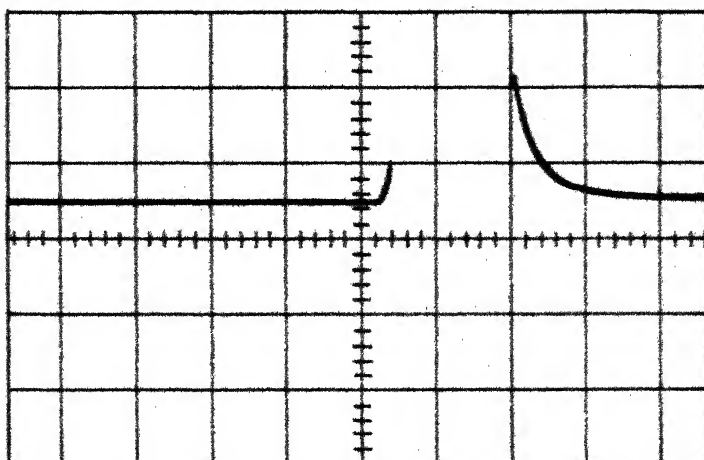
Fig.4.3(a)- Laser schlieren signal in pure SO_2.

Time scale: $2\mu S/cm$

$p_1 = 1.76$ torr; $T_2 = 716\ °K$

$u_S = 0.784\ mm/\mu S$

$\gamma_L = 0.874\mu S$
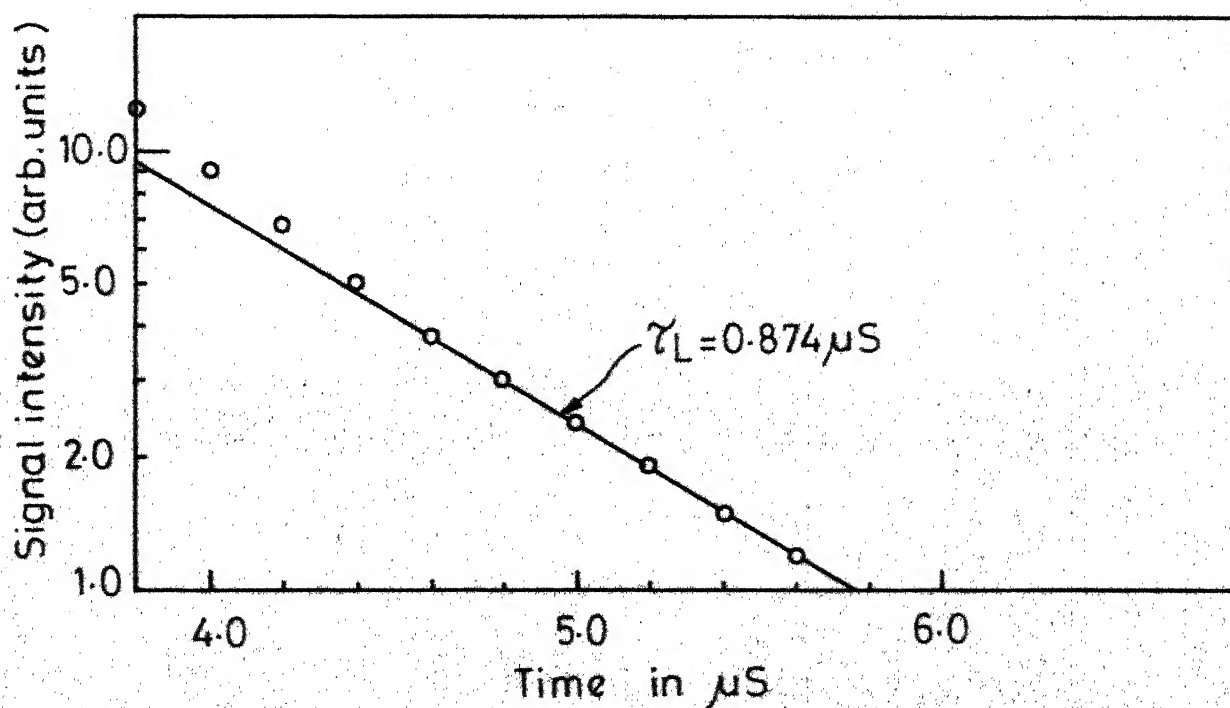
Fig.4.3(b)-Semi-log plot of fig. 4.3 (a).

To verify whether the observed times are really due to relaxation or not, a few experiments are conducted with mixtures of 10% n-Hexane and 90% SO_2. The addition of such small quantities of n-Hexane has very little effect on the physical properties of SO_2 but considerably reduces the relaxation times[15]. It is found that the relaxation times obtained in these mixtures are always equal to the detector response time, indicating that the measured times in SO_2 are indeed due to vibrational relaxation. If this were not the case then no difference would have been found between the signals obtained in pure SO_2 and SO_2-n-Hexane mixtures.

Table 4.2 summarizes the results obtained in pure SO_2. The relaxation times are plotted on a Landau-Teller plot ($\log P\tau$ vs $T^{-1/3}$) in fig.4.4. The straight line in fig.4.4 is a least squares fit to the present data and is given by the following equation.

$$P\tau = \exp(-2.713 + 9.3\ T^{-1/3}); \quad \sigma = 12\% \qquad (4.1)$$

where $P\tau$ = relaxation time in μS at 1 atm.

and σ = standard deviation in $P\tau$.

The black circles in fig.(4.4) correspond to measurements made on SO_2 purified in the manner described earlier. The open circles correspond to SO_2 taken directly from the cylinder.

Table No. 4.2

Vibrational relaxation data in SO_2

S.No.	p_1 (mmHg)	u_s (mm/μS)	T_2 (°K)	τ_L (μS)	$P\tau$ (atm. μS)
1	1.36	0.850	781.1	0.552	0.164
2	1.76	0.784	714.7	0.874	0.259
3	2.48	0.824	757.2	0.478	0.237
4	1.20	0.921	860.8	0.626	0.213
5	1.00	0.867	802.5	0.713	0.168
6	1.08	0.913	851.4	0.617	0.184
7	1.04	0.952	895.7	0.526	0.171
8	1.02	0.985	933.8	0.500	0.176
9	0.72	1.097	1072.0	0.459	0.158
10	0.61	1.131	1117.1	0.472	0.149
11	1.60	0.818	750.9	0.584	0.182
12	1.44	0.821	753.1	0.584	0.166
13	1.56	0.696	633.4	1.025	0.183
14	1.64	0.795	727.6	0.605	0.177
15	2.08	0.697	634.1	0.800	0.193
16	2.00	0.695	632.2	0.830	0.190
17	2.52	0.739	672.9	0.595	0.210
18	2.88	0.708	643.5	0.613	0.214
19	2.16	0.661	601.7	0.826	0.172
20	0.80	1.121	1103.8	0.383	0.156

Table No. 4.2 (Contd.)

Vibrational relaxation data in SO_2

S.No.	p_1 (mmHg)	u_s (mm/μS)	T_2 ($^\circ$K)	τ_L (μS)	$P\tau$ (atm.μS)
21	0.90	1.077	1045.4	0.495	0.202
22	1.00	0.994	945.0	0.426	0.152
23	0.96	1.040	1000.7	0.396	0.155
24	0.64	1.187	1192.8	0.387	0.149
25	1.88	0.612	560.0	1.335	0.186
26	1.70	0.713	648.1	0.922	0.196
27	1.68	0.679	617.5	0.982	0.174
28	0.91	1.039	1000.0	0.400	0.148
29	1.12	0.940	882.1	0.535	0.181
30	1.16	0.924	862.2	0.539	0.178
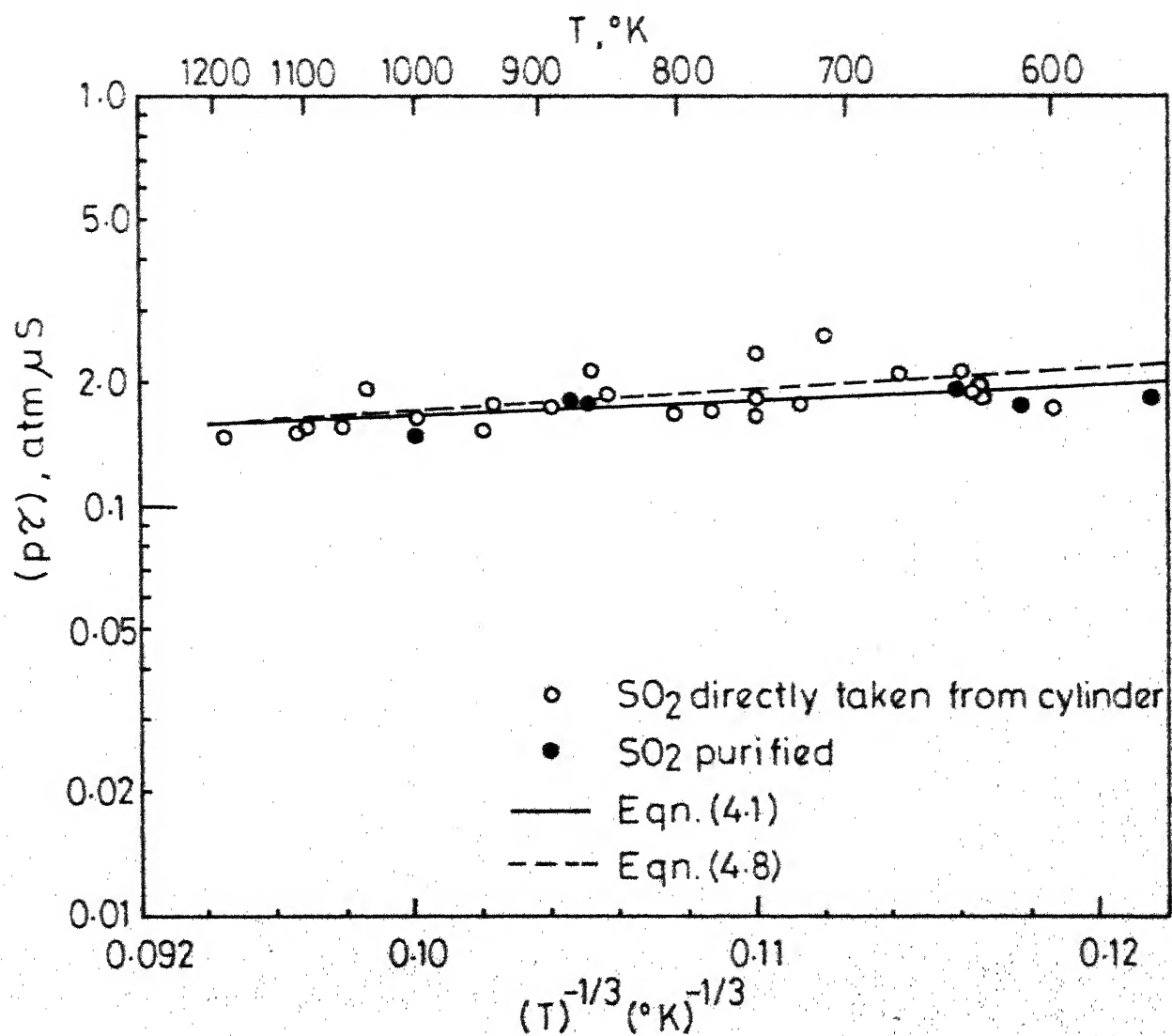
Fig. 4.4 – Vibrational relaxation times in pure SO_2.

IV.3 MIXTURES OF SO_2 AND ARGON

Vibrational relaxation times are obtained for three different compositions in mixtures of SO_2 and Argon, namely i) 54% SO_2, ii) 20% SO_2 and iii) 11% SO_2. The temperature ranges covered for these mixtures are 758°K - 1840°K, 809°K-2126°K, and 777°K - 2018°K respectively. The density gradient profiles in most cases are similar to those obtained in pure SO_2, the initial points deviating from straight line plots. As the peak of the schlieren records lies very much off the scale, precise information regarding the processes that cause the deviation in the immediate vicinity of the shock front could not be obtained in many runs. However, a few runs in 20% and 11% mixtures are conducted (5 runs with each composition) in which the vertical scale of the schlieren records has been compressed by a factor of 4 so that the entire spike is visible. Two oscilloscopes are employed for this purpose. The vertical scales in the plug-in units of the two scopes differ by a factor of 4. A typical record thus obtained is shown in fig.(4.5). It can be clearly seen from this figure that for the record in which the full spike is visible, the falling portion of the signal can be divided into two separate parts, one in which the relaxation processes are fast and other in which the relaxation processes are slow.
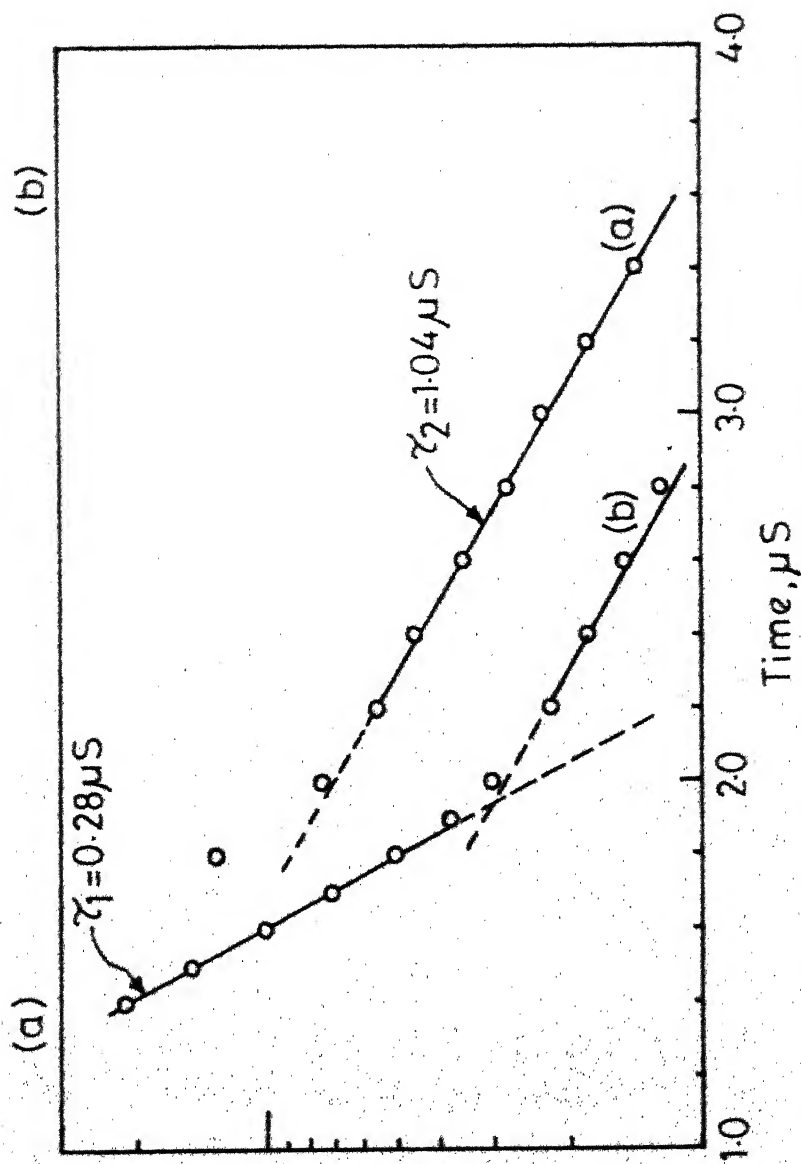
Fig. 4.5 - Laser schlieren signals and the corresponding semi-log plots for a sample run in 11.0% SO_2-Ar mixture.

It can be further noted that the relaxation in both regions follows exponential behaviour describable by two different time constants τ_1 and τ_2. The reason for the absence of double exponential behaviour in 70% of the runs in pure SO_2 can be that the initial process is too fast to be recorded effectively by the oscilloscope.

One might argue that the break in the slopes signifies the departure of the shock front from the laser beam. If this were the case, then the naperian time (inverse slope of the corresponding semi-log plot) τ_1 of the fast process should be approximately equal to the over-all response time of the system as obtained in pure Argon. But it is found that the former time is at least three times that of the latter. These observations strongly suggest that the relaxation in sulfur dioxide and sulfur dioxide-Argon mixtures follows a double exponential path. However, quantitative measurements for the fast process have not been attempted chiefly because of the difficulty in ascertaining any single value of density or temperature in this region. The region in the immediate vicinity of the shock front is characterized by rapidly changing values of density, temperature etc. Hence in the evaluation of particle relaxation times by eq.(3.12) no single value of ρ or C_p can be used and the relaxation time cannot be ascribed to any single temperature.

The results for the slow process in the three SO_2-Ar mixtures are summarized in Tables (4.3), (4.4) and (4.5). The corresponding Landau-Teller plots are shown in figs. (4.6), (4.7) and (4.8). The solid lines in these figures are the least squares fits of the data given by the following equations:

$$(P\tau)_{11\%} = \exp(-4.26 + 35.4T^{-1/3}) \; ; \; \sigma = 13\% \qquad (4.2)$$

$$(P\tau)_{20\%} = \exp(-3.78 + 26.9 \, T^{-1/3}) \; ; \sigma = \; 7\% \qquad (4.3)$$

$$(P\tau)_{54\%} = \exp(-3.74 + 25.1 \, T^{-1/3}) \; ; \sigma = \; 9\% \qquad (4.4)$$

Shields[16] assumed that the relaxation times in the SO_2-raregas mixtures obey the mixture rule[2]

$$\frac{1}{(P\tau)}_{mix} = \frac{X}{(P\tau)}_{SO_2-SO_2} + \frac{1-X}{(P\tau)}_{SO_2-M} \qquad (4.5)$$

where $(P\tau)_{mix}$ = relaxation time at 1 atm.for the mixture

$(P\tau)_{SO_2-SO_2}$ = relaxation time at 1 atm.for SO_2

$(P\tau)_{SO_2-M}$ = relaxation time at 1 atm.for SO_2

infinitely diluted in the rare gas M

and X = mole fraction of SO_2 in the mixture.

The temperature dependence of the relaxation times in the various mixtures suggest that $(P\tau)_{SO_2-SO_2}$ and $(P\tau)_{SO_2-Ar}$ can be expressed by equations similar to eqs.(4.2)-(4.4).

Table No. 4.3

Vibrational relaxation data in 54% SO_2 + Ar mixture

S.No.	p_1 (mmHg)	u_s (mm/μS)	T_2 (°K)	τ_L (μS)	$P\tau$ (atm.μS)
1	3.52	0.825	795.0	0.890	0.326
2	3.32	0.854	830.0	0.816	0.314
3	3.16	0.910	897.2	0.656	0.290
4	2.74	0.947	945.0	0.621	0.269
5	2.56	1.028	1054.8	0.582	0.298
6	2.16	1.055	1089.2	0.538	0.249
7	2.22	1.108	1169.0	0.465	0.252
8	1.98	1.191	1296.0	0.434	0.259
9	2.22	1.158	1245.0	0.391	0.241
10	1.32	1.328	1522.4	0.412	0.220
11	1.40	1.383	1620.9	0.330	0.208
12	0.80	1.500	1840.0	0.378	0.168
13	0.80	1.471	1780.0	0.450	0.191
14	2.06	1.235	1368.0	0.321	0.220
15	4.48	0.793	758.0	0.994	0.409
16	3.34	0.892	876.0	0.847	0.373
17	2.56	0.950	949.2	0.855	0.349

Table No. 4.4

Vibrational relaxation data in 20% SO_2 + Ar mixture

S.No.	p_1 (mmHg)	u_s (mm/μS)	T_2 (°K)	τ_L (μS)	$P\tau$ (atm.μS)
1	8.14	0.846	866.6	0.908	0.409
2	7.52	0.821	834.6	1.050	0.400
3	9.44	0.802	809.8	0.886	0.397
4	7.28	0.830	845.4	0.842	0.322
5	7.12	0.907	954.8	0.734	0.353
6	5.92	0.966	1043.8	0.699	0.333
7	4.66	1.046	1173.6	0.621	0.289
8	3.64	1.159	1368.8	0.547	0.261
9	4.52	1.084	1236.7	0.595	0.295
10	3.52	1.242	1502.6	0.460	0.248
11	2.48	1.299	1639.0	0.486	0.211
12	2.08	1.331	1706.0	0.565	0.219
13	1.52	1.521	2126.6	0.480	0.190
14	1.52	1.444	1947.8	0.504	0.174
15	1.72	1.459	1984.0	0.447	0.180
16	2.37	1.322	1684.0	0.517	0.224
17	1.92	1.295	1630.6	0.712	0.238
18	6.72	0.854	879.3	0.990	0.378
19	4.88	0.960	1034.3	0.895	0.346
20	4.52	1.021	1130.3	0.721	0.304
21	1.48	1.190	1426.3	1.240	0.257
22	1.64	1.111	1283.0	1.550	0.300

Table No. 4.5

Vibrational relaxation data in 11% SO_2 + Ar mixture

| S.No.	p_1(mmHg)	u_s(mm/μS)	T_2(°K)	τ_L(μS)	$P\tau$ (atm.μS)
1	11.20	0.771	777.0	1.650	0.619
2	9.16	0.856	897.0	1.607	0.658
3	10.32	0.816	840.0	1.790	0.725
4	8.08	0.913	985.0	1.240	0.535
5	8.16	0.946	1035.0	0.830	0.398
6	7.12	0.984	1099.6	0.851	0.395
7	5.52	1.112	1325.0	0.725	0.360
8	5.40	1.131	1360.0	0.560	0.284
9	5.64	1.106	1314.0	0.868	0.433
10	3.96	1.215	1527.0	0.803	0.357
11	2.16	1.438	2018.0	0.721	0.264
12	2.16	1.435	2008.0	0.782	0.284
13	2.60	1.413	1960.0	0.569	0.240
14	3.48	1.275	1649.0	0.612	0.270
15	2.74	1.300	1703.0	0.621	0.226
16	3.06	1.243	1585.0	0.770	0.280
17	3.96	1.214	1527.0	0.621	0.276
18	4.00	1.212	1520.0	0.634	0.283
19	3.68	1.151	1400.0	0.860	0.310
20	5.60	1.053	1217.0	0.873	0.382
21	4.98	1.063	1235.0	1.042	0.414
22	6.64	0.952	1047.0	1.130	0.449
23	9.38	0.847	884.0	1.282	0.522
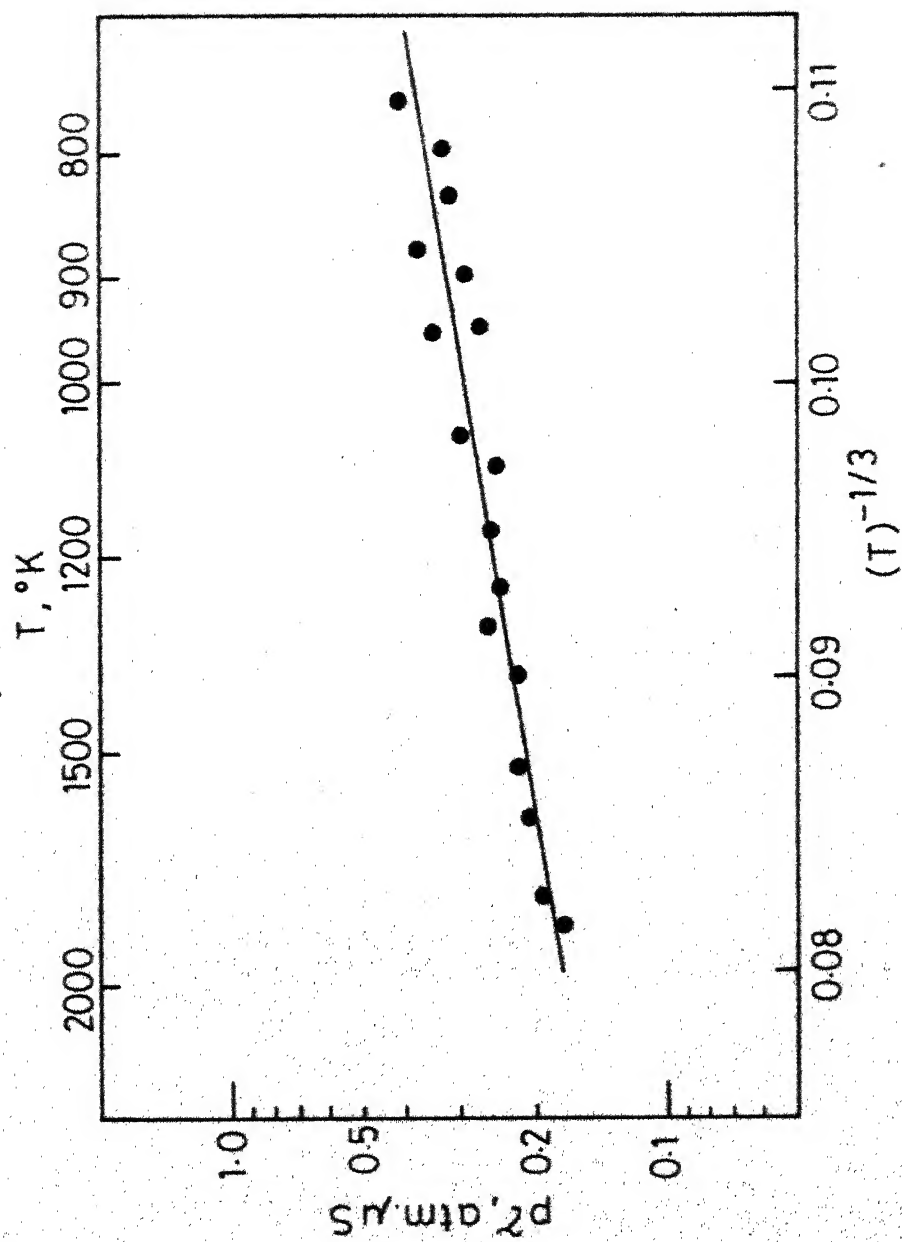
Fig. 4.6—Vibrational relaxation times in 54 % SO2 + Ar mixture.
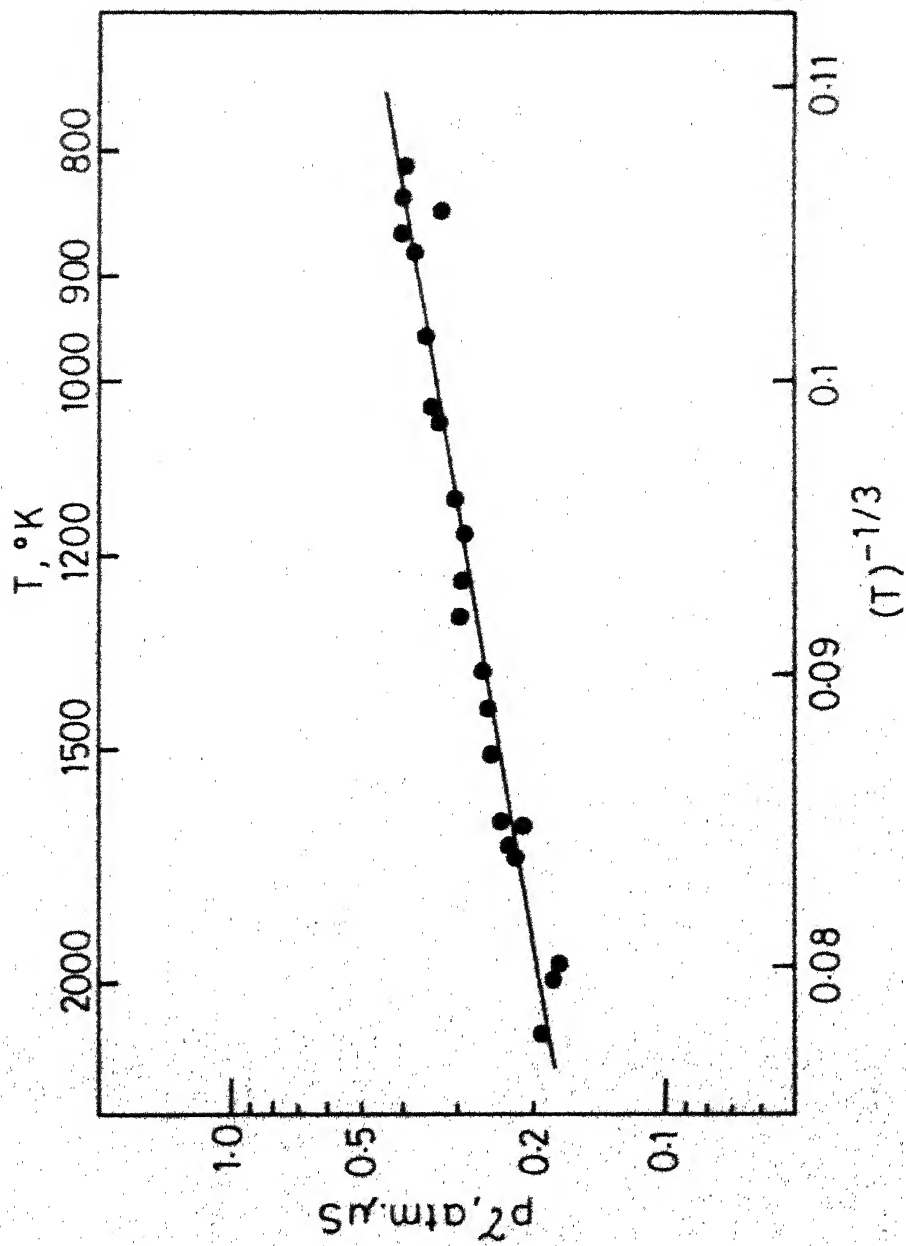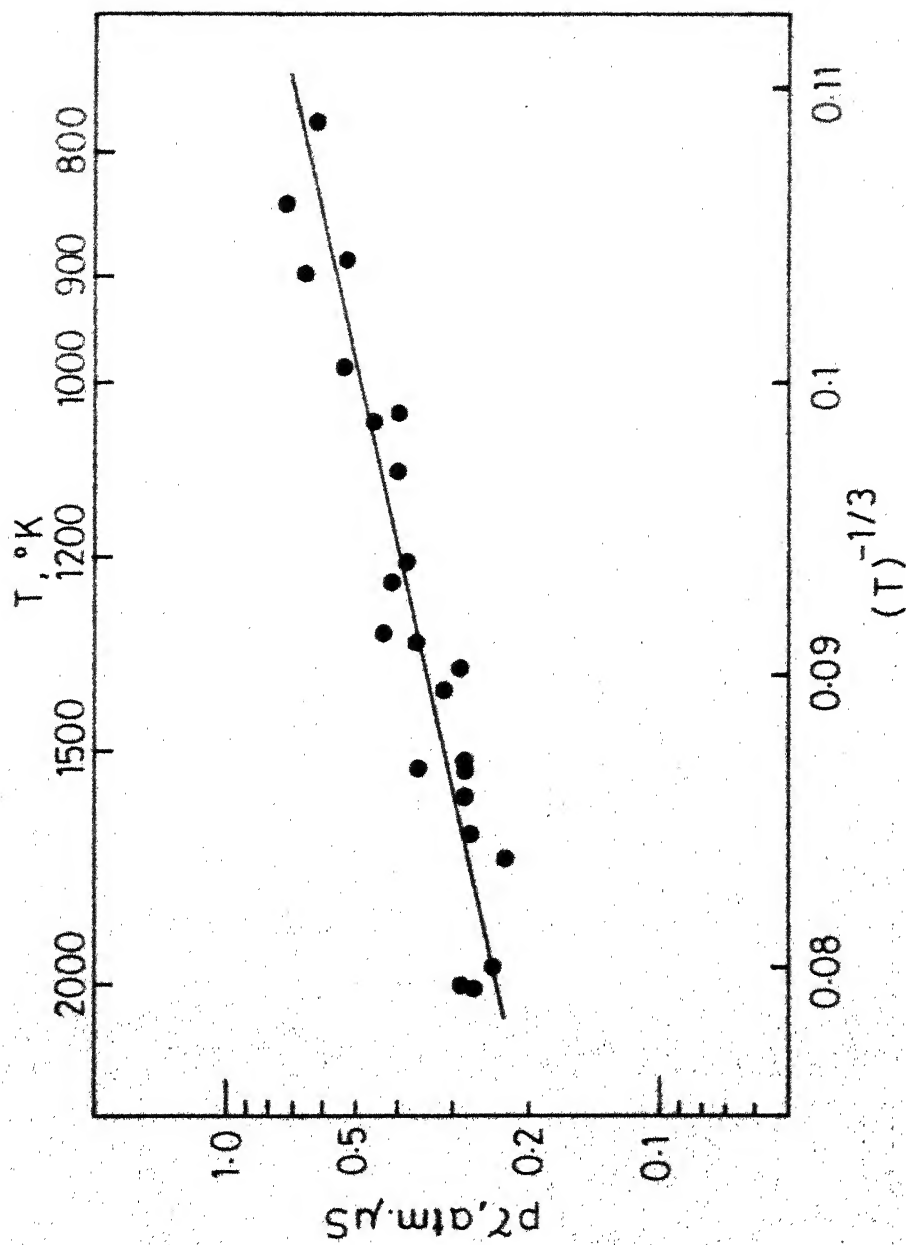
Fig. 4.7 – Vibrational relaxation times in 20 % SO₂ + Ar mixture.

Fig. 4.8 – Vibrational relaxation times in 11.0% SO_2+Ar mixture.

So it can be written that

$$(P\tau)_{SO_2-SO_2} = \exp(A+BT^{-1/3}) \qquad (4.6)$$

and

$$(P\tau)_{SO_2-Ar} = \exp(C+DT^{-1/3}) \qquad (4.7)$$

A computer programme is written to evaluate the best values of A,B,C and D by a least squares analysis using the data for all the mixtures including 100% SO_2, eqs.(4.5), (4.6) and (4.7) and the mole fraction X as the input. The following equations for $(P\tau)_{SO_2-SO_2}$ and $(P\tau)_{SO_2-Ar}$ are obtained from such analysis.

$$(P\tau)_{SO_2-SO_2} = \exp(-2.965 + 11.9\ T^{-1/3}) \qquad (4.8)$$

$$(P\tau)_{SO_2-Ar} = \exp(-4.65 + 40.32\ T^{-1/3}) \qquad (4.9)$$

In obtaining equations (4.8) and (4.9), $(P\tau)$ values in pure SO_2 below 700°K are not included in the analysis so that the same low temperature limit can be maintained for all the compositions. Eq.(4.8) is only slightly different from eq.(4.1), as can be seen from fig.(4.4) in which eq.(4.1) is shown as the solid line and eq.(4.8) is shown as the dashed line. However, eq.(4.8) is taken to be more appropriate because it is obtained over a wider temperature range and using a larger number of data points.

In the above analysis, $(P\tau)_{SO_2-SO_2}$ and $(P\tau)_{SO_2-Ar}$
have been obtained assuming that the mixture rule holds good.
To verify how well the mixture rule is obeyed, $(1/P\tau)_{mix}$ is
plotted against X in fig.(4.9). The solid line in this figure
is given by eq.(4.5) with eqs.(4.8) and 4.9). The values of
$(P\tau)$ are evaluated at 1000°K. The black circles correspond
to values obtained from eqs.(4.1) – (4.4). It can be seen
from this figure that the maximum deviation from mixture rule
is about 20%, showing that the mixture rule is obeyed fairly
well.

The error bars given in fig.(4.9) correspond to the
percentage errors defined as

$$P_X^2 = \frac{1}{N} \sum_N \left\{ \frac{(P\tau)_{exp} - (P\tau)_{calc}}{(P\tau)_{calc}} \right\}^2$$

where P_X = percentage error for the mixture of composition X

N   = total number of points for the given mixture

$(P\tau)_{exp}$ = experimental values of $(P\tau)$ for the mixture

and $(P\tau)_{calc}$ = values of $(P\tau)$ calculated from eqs.(4.5),
(4.8) and (4.9).

The values of P_X for X = 0.11, 0.20 and 0.54 are 17.8%,
10.4% and 19.7% respectively. The values of P_X for 0% and
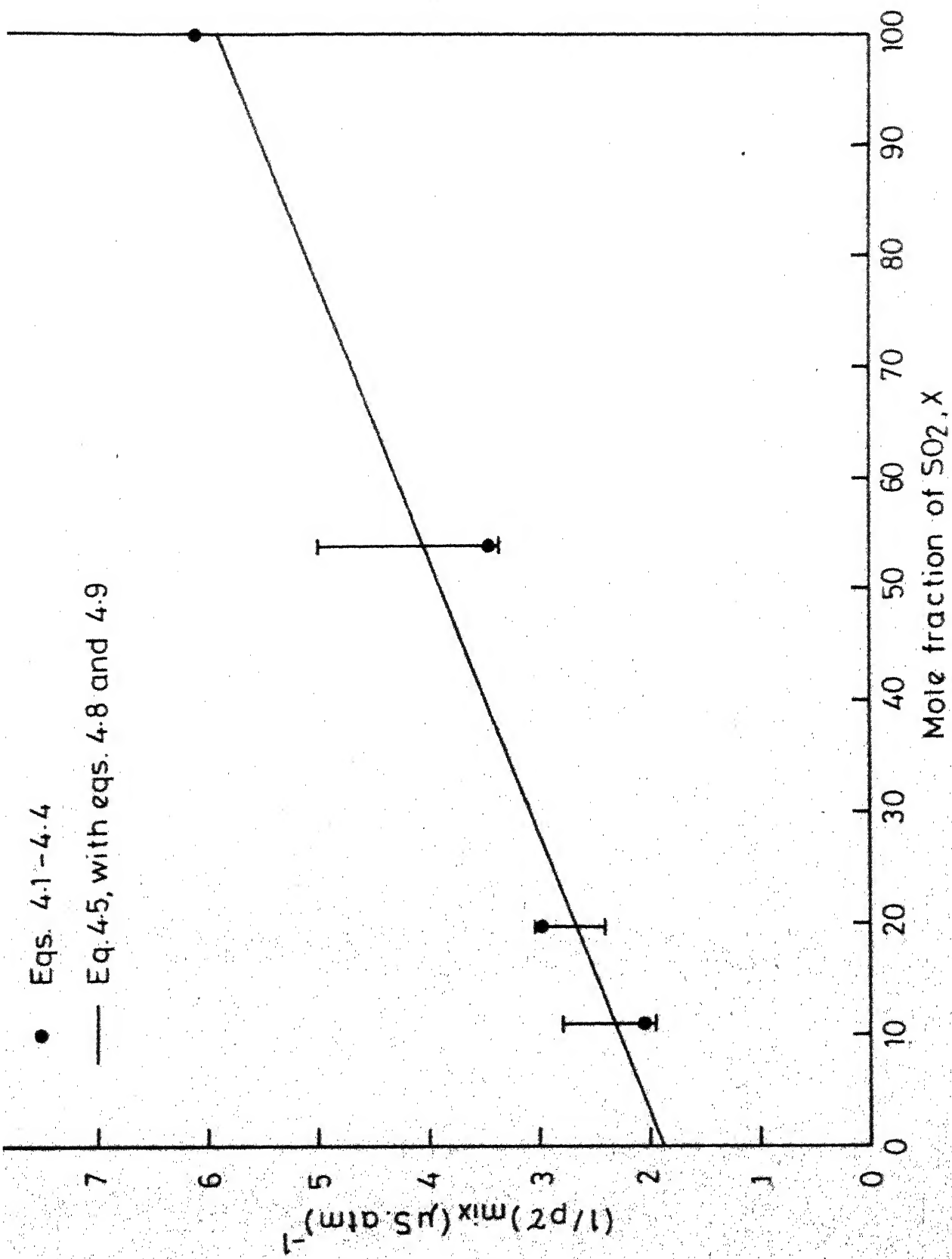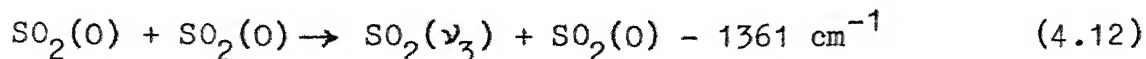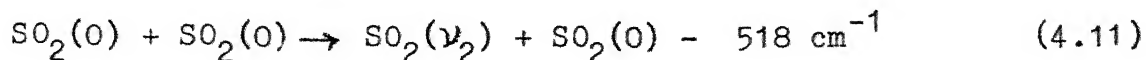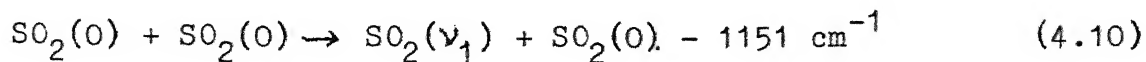100% SO_2 have been obtained by extending the envelope of the

Fig.4.9 - $(p\tau)^{-1}$ vs. mole fraction of SO_2 in SO_2-Ar

error bars given in fig.(4.9) graphically to the 0% and 100% intercepts. The values thus obtained are shown in figs.(4.12) and (4.13).

IV.4 <u>MECHANISM OF ENERGY TRANSFER IN SO_2</u>

All the ultrasonic studies in SO_2 indicate the presence of a double dispersion behaviour. This had been explained by a mechanism in which the lowest vibrational mode ν_2 (see fig. 4.10) is first activated by a fast T-V process followed by a relatively slow activation of the rest of the vibrational modes, ν_1 and ν_3. To understand these processes further, it is necessary to consider which of the mechanisms - parallel or series mechanism - is responsible for the excitation. These two mechanisms are discussed below.

i)   parallel mechanism : If the vibrational relaxation in SO_2 is assumed to proceed by a parallel process, then, as discussed in Chapter II, the individual vibrational modes would be activated by T-V processes like

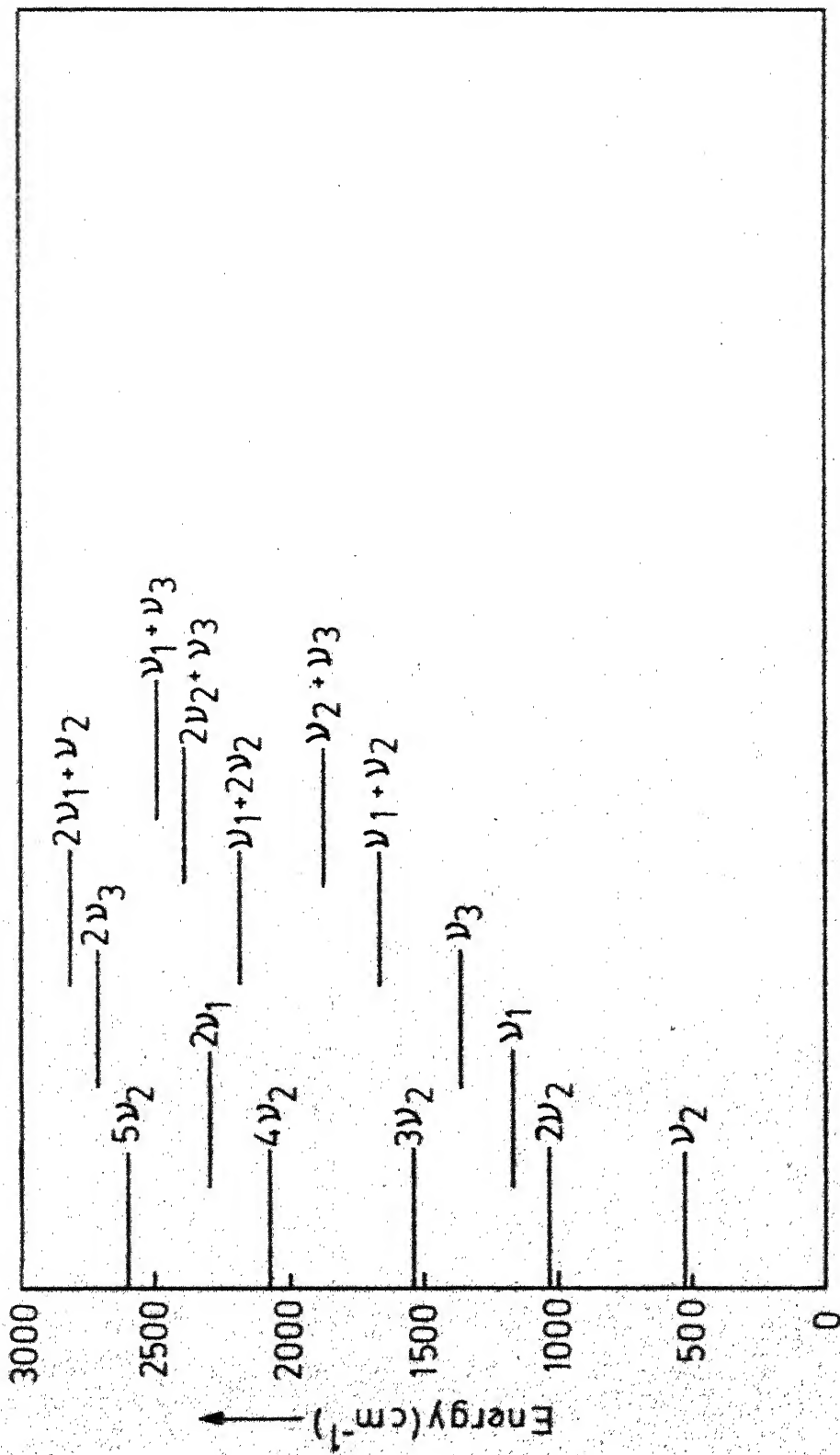$$SO_2(0) + SO_2(0) \rightarrow SO_2(\nu_1) + SO_2(0) - 1151 \text{ cm}^{-1} \qquad (4.10)$$

$$SO_2(0) + SO_2(0) \rightarrow SO_2(\nu_2) + SO_2(0) - 518 \text{ cm}^{-1} \qquad (4.11)$$

$$SO_2(0) + SO_2(0) \rightarrow SO_2(\nu_3) + SO_2(0) - 1361 \text{ cm}^{-1} \qquad (4.12)$$

Energy (cm⁻¹) axis labels:

$5\nu_2$
$2\nu_1 + \nu_2$
$2\nu_3$
$\nu_1 + \nu_3$
$2\nu_2 + \nu_3$
$2\nu_1$
$\nu_1 + 2\nu_2$
$4\nu_2$
$\nu_2 + \nu_3$
$\nu_1 + \nu_2$
$3\nu_2$
ν_3
ν_1
$2\nu_2$
ν_2

Energy (cm⁻¹)

3000 2500 2000 1500 1000 500 0

Fig.4.10 - Partial energy level diagram of SO_2.

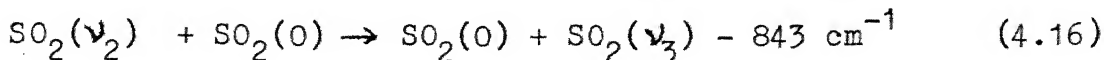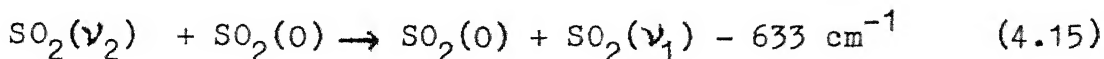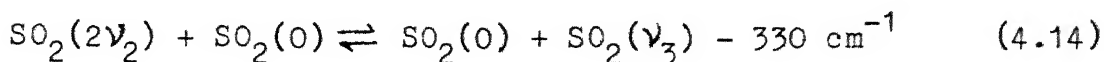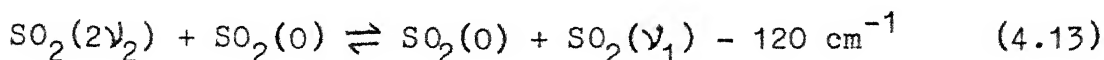Here $SO_2(0)$ represents an SO_2 molecule in the ground vibrational state and $SO_2(\nu_i)$. (i = 1,2,3), represents an SO_2 molecule in the first vibrational level of the ith mode. Molecules in the second level of mode i will be represented as $SO_2(2\nu_i)$, etc.

Then, the fast process in the ultrasonic studies must be due to reaction (4.11) and the slow process must be due to reactions (4.10) and (4.12). The latter processes are necessarily slower since they require the absorption of more than double the energy of (4.11) from translation.

ii) series mechanism : In this mechanism the ν_2 mode will still be excited by the T-V process (4.11), but the subsequent excitation of ν_1 and ν_3 modes proceeds by V-V processes like

$$SO_2(2\nu_2) + SO_2(0) \rightleftharpoons SO_2(0) + SO_2(\nu_1) - 120 \text{ cm}^{-1} \qquad (4.13)$$

$$SO_2(2\nu_2) + SO_2(0) \rightleftharpoons SO_2(0) + SO_2(\nu_3) - 330 \text{ cm}^{-1} \qquad (4.14)$$

$$SO_2(\nu_2) + SO_2(0) \longrightarrow SO_2(0) + SO_2(\nu_1) - 633 \text{ cm}^{-1} \qquad (4.15)$$

$$SO_2(\nu_2) + SO_2(0) \longrightarrow SO_2(0) + SO_2(\nu_3) - 843 \text{ cm}^{-1} \qquad (4.16)$$

$$SO_2(\nu_1) + SO_2(0) \rightleftharpoons SO_2(0) + SO_2(\nu_3) - 210 \text{ cm}^{-1} \qquad (4.17)$$
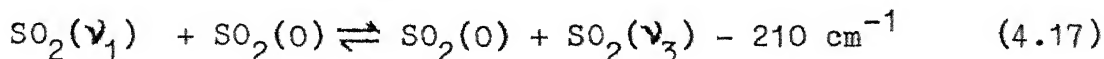
If this series mechanism is assumed then the slow process of ultrasonic studies must be due to reactions (4.13)-(4.17).

Theoretical studies of Dickens and Linnette[19] suggest that a series process is most likely to predominate in SO_2 relaxation. Their calculations also indicate that only the transition probabilities for reactions (4.11),(4.13) and (4.17) are large enough to warrant consideration. Shields[16] studied mixtures of SO_2 and Argon (100%, 75% and 50% SO_2) at three temperatures, 300°K, 400°K and 500°K by the ultrasonic method and observed that the experimental data could be fitted with theoretical curves for series and parallel processes alike. Later, with improvements in apparatus and using a 25% SO_2+Ar mixture, Shields and Anderson[17] found that the theoretical curves obtained assuming the series mechanism give a better fit to the experimental data than the theoretical curves obtained for the parallel mechanism. Siebert and Flynn[22] observed laser induced fluorescence at 7.5 μ from ν_3 state at 300°K by using a Q-switched CO_2 laser to excite the ν_1 level of SO_2. The rate of rise of the fluorescence signals gave a measure of the rate at which the ν_1 and ν_3 levels equilibrate, and was found to be fast ($\sim$300 collisions). The rate of fall of the fluorescence signals was very close to the slower rates obtained in the ultrasonic studies at room temperature. By studying the variation of this rate with reduced mass in mixtures of SO_2 with He, Ne, Ar and Kr, they concluded that the fall of the

fluorescence signals was due to V-V processes rather than V-T deactivation of the ν_3 level, and that the reaction (4.13) is chiefly responsible for the fall of the fluorescence signals.

Based on these observations Siebert and Flynn[22] concluded that the most probable scheme for vibrational excitation in SO_2 seems to be the following at room temperature.

i)   The ν_2 mode is first activated by a fast T-V process.

ii)   The ν_1 mode is then activated by a slow V-V energy exchange with $2\nu_2$.

iii) The ν_3 mode equilibrates with the ν_1 mode by a fast V-V energy transfer processes.

Our results at high temperatures also seem to be consistent with the series mechanism. Process(iii) above was found to show the Landau-Teller temperature dependence, its rate increasing with temperature upto 500°K[16], and it may be expected to continue increasing at higher temperatures. So the assumption that the ν_1 and ν_3 modes are locked together by a fast V-V processeseems reasonable at higher temperatures also. Further, Bass et al[18] studied relaxation in pure SO_2 upto 1100°K by the ultrasonic method and found that the collision number Z_{10} for process (i) is smaller than the collision

number $Z_{2,3}$ for process(ii) for temperatures upto 1100°K.
These collision numbers are defined as follows:

$$Z_{10} = Z \beta_1 \{1 - \exp(-h\nu_2/kT)\} \qquad (4.18)$$

$$Z_{2,3} = Z \beta_2 \{1 - \exp(-h\nu_1/kT)\} \qquad (4.19)$$

where Z = no of collisions per second at the given tempe-
rature T and 1 atm. pressure,

β_1 = the relaxation time at 1 atm. for the excitation
of the ν_2 mode,

$\beta_2 = \tau_2 \cdot \dfrac{C_{\nu_1}}{C_{\nu_1} + C_{\nu_2}}$, τ_2 being the relaxation time

at 1 atm. for the excitation of the $\nu_1 - \nu_3$ modes
and C_{ν_i} the vibrational specific heat of the ith
mode.

Theoretical calculations[35] show that Z_{10} decreases faster
above 800°K than in the region below 800°K, suggesting that
Z_{10} is less than $Z_{2,3}$ for temperature above 1100°K also.
All these observations suggest that the relaxation mechanism
proposed above at room temperature is valid at higher tempe-
rature also.

The results of the present investigation can be inter-
preted in the light of the above relaxation scheme. It should

first be seen whether the density changes accompanying the vibrational excitation of ν_1 and ν_3 modes are measurable or not. As the contribution to the density change from various modes is through the vibrational specific heat, this can be done by evaluating the relative contributions from each mode to the total vibrational specific heat as a function of temperature. This is shown in fig.(4.11). It can be seen that the contribution of the ν_1 mode is quite significant in comparison to that of the ν_2 mode. At temperatures as low as 550°K, the contribution from ν_1 and ν_3 together is about equal to the contribution from the ν_2 mode. This suggests that the density changes accompanying the vibrational excitation of ν_1 and ν_3 modes are large enough to be measured. Further, since the specific heat contributions from the ν_1 and ν_3 modes were large enough to be detected by ultrasonic techniques, it should be so, for shock tube studies also.

Hence, the initial fast process observed in the schlieren records of the present study can be interpreted as the activation of the ν_2 mode and the slower process as the activation of ν_1 and ν_3 modes. To make a comparison of the present results with those of earlier works, the present values of $(P\tau)_{SO_2-SO_2}$ are plotted in fig.(4.12) together with the $\tau_{2,3}$ values of Shields[16] and Bass et.al[18] and the slower
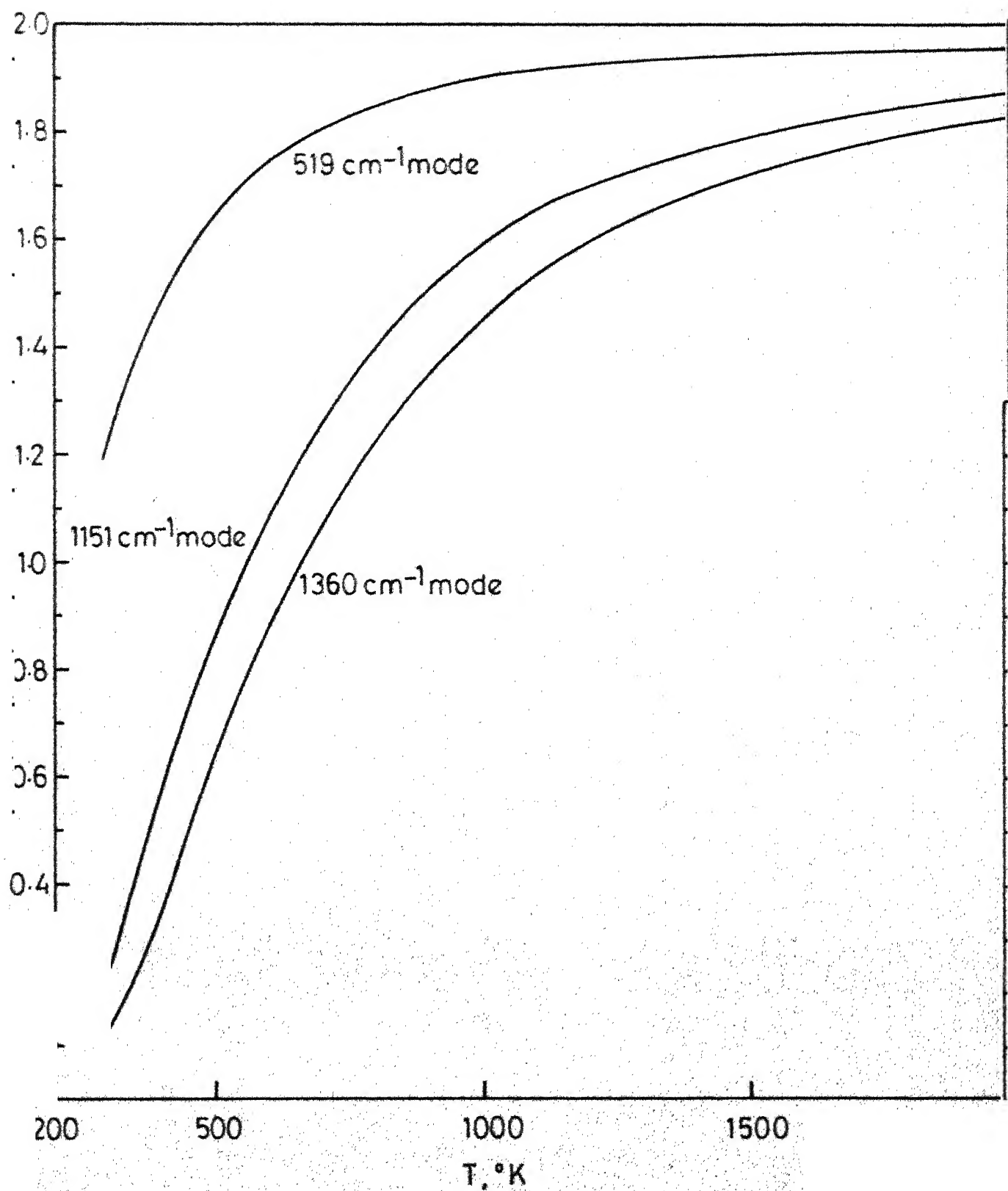
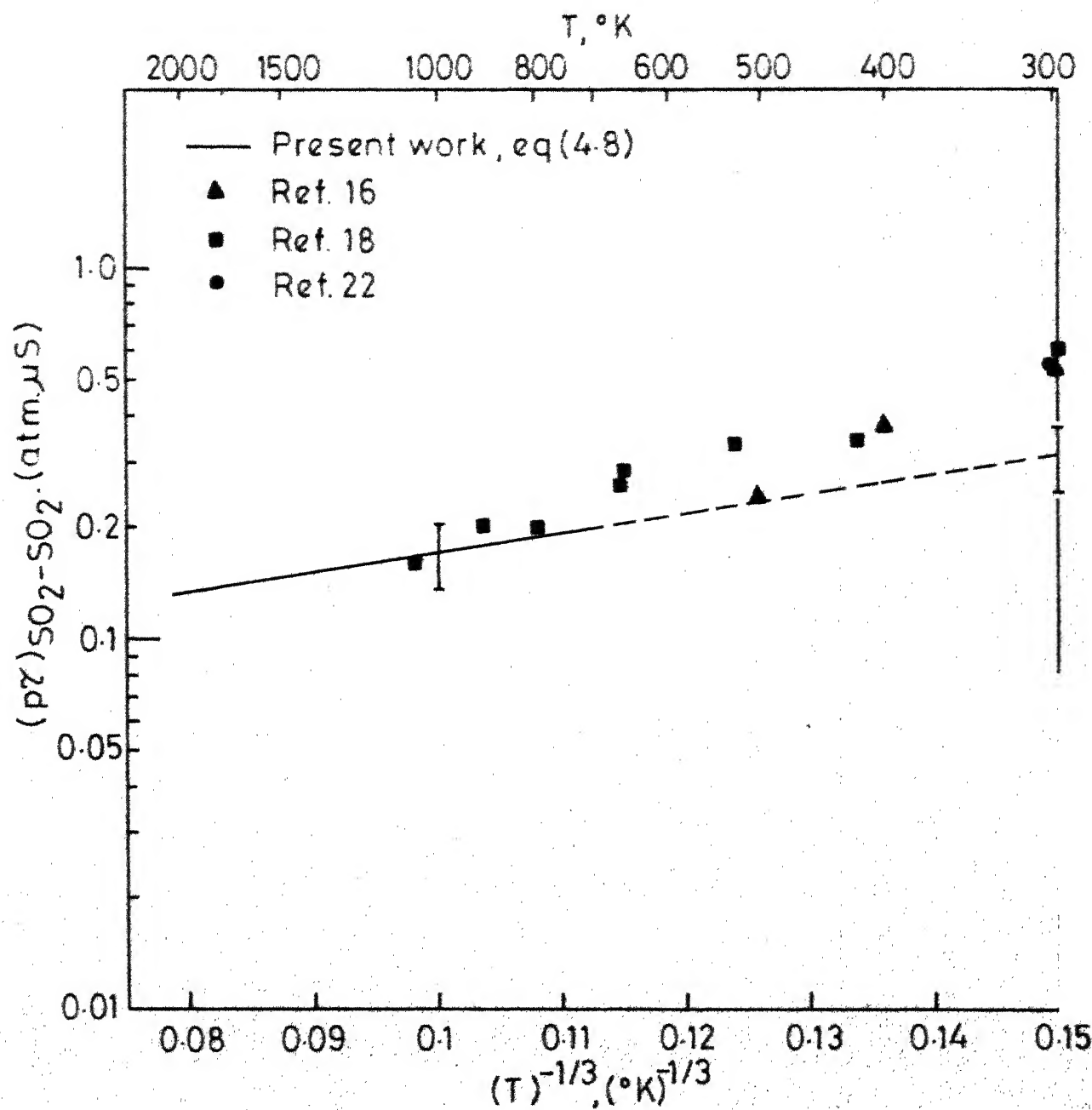Fig 4.11 – Variation of specific heats of different vibrational modes of SO_2 with temperature.

Fig. 4·12 – Vibrational relaxation times in pure SO_2.

fall time of the laser induced fluorescence studies. The solid line for $(P\tau)_{SO_2-SO_2}$ is given by eq.(4.8) and the dashed line in the extrapolation of eq.(4.8) to room temperature. It is seen from this figure that the present results are in good agreement with those of ultrasonic and laser fluorescence studies. The temperature dependence obtained in this study is slightly different from that of earlier works. The present values of $(P\tau)_{SO_2-Ar}$ are also compared with the slower rates of ultrasonic and laser induced fluorescence studies in fig.(4.13). Again it can be seen that the comparison is good.

IV.5 THE SO_2-He SYSTEM

Relaxation times of SO_2 in the presence of Helium are also measured in this study in the temperature range 700°K – 1600°K. Measurements have been made in a mixture of 9.5% SO_2+He. Because of the low density of Helium, the schlieren signals are found to be weak, resulting in a larger scatter in the data than for the SO_2-Ar system. The presence of a double relaxation can be seen here also, as shown in fig.(4.14). The results of 9.5% SO_2-He mixture are summarized in Table 4.6 and shown in Fig.(4.15). The relaxation times of SO_2 infinitely diluted in He are obtained by using the mixture rule (4.5) with $(P\tau)_{SO_2-SO_2}$ given by eq.(4.8) and
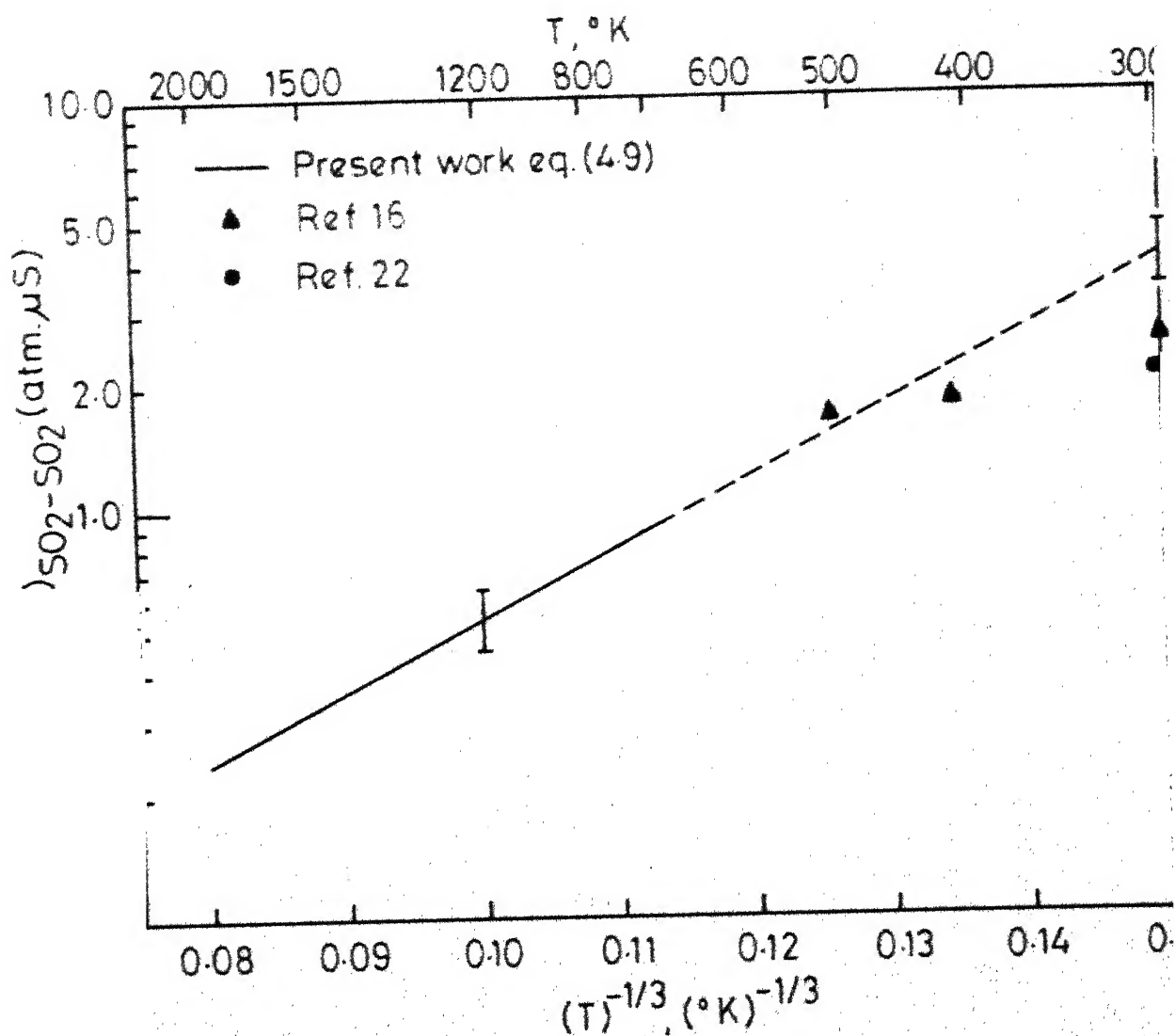
Fig. 4.13–Vibrational relaxation times of SO_2 infinitely diluted in Argon.

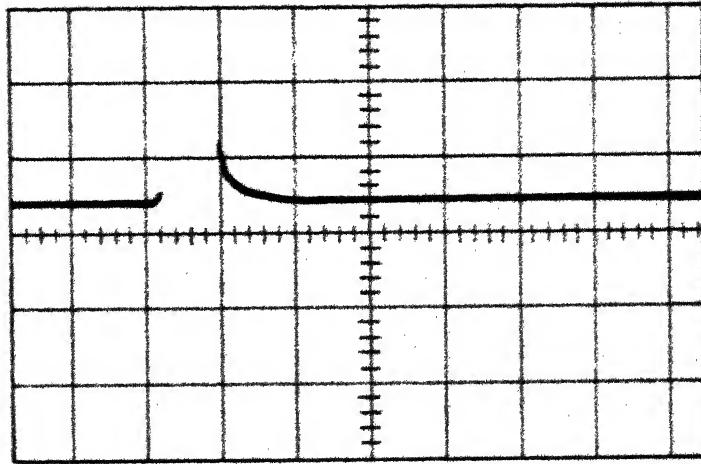Fig.4.14(a)– Laser schlieren signal in 9.5% SO_2–He mixture.
$p_1 = 8.32$ torr, $u_S = 1.663$ mm/μS, $T_2 = 820\,°K$.
sweep rate $= 2\mu S/cm$

Time, μS
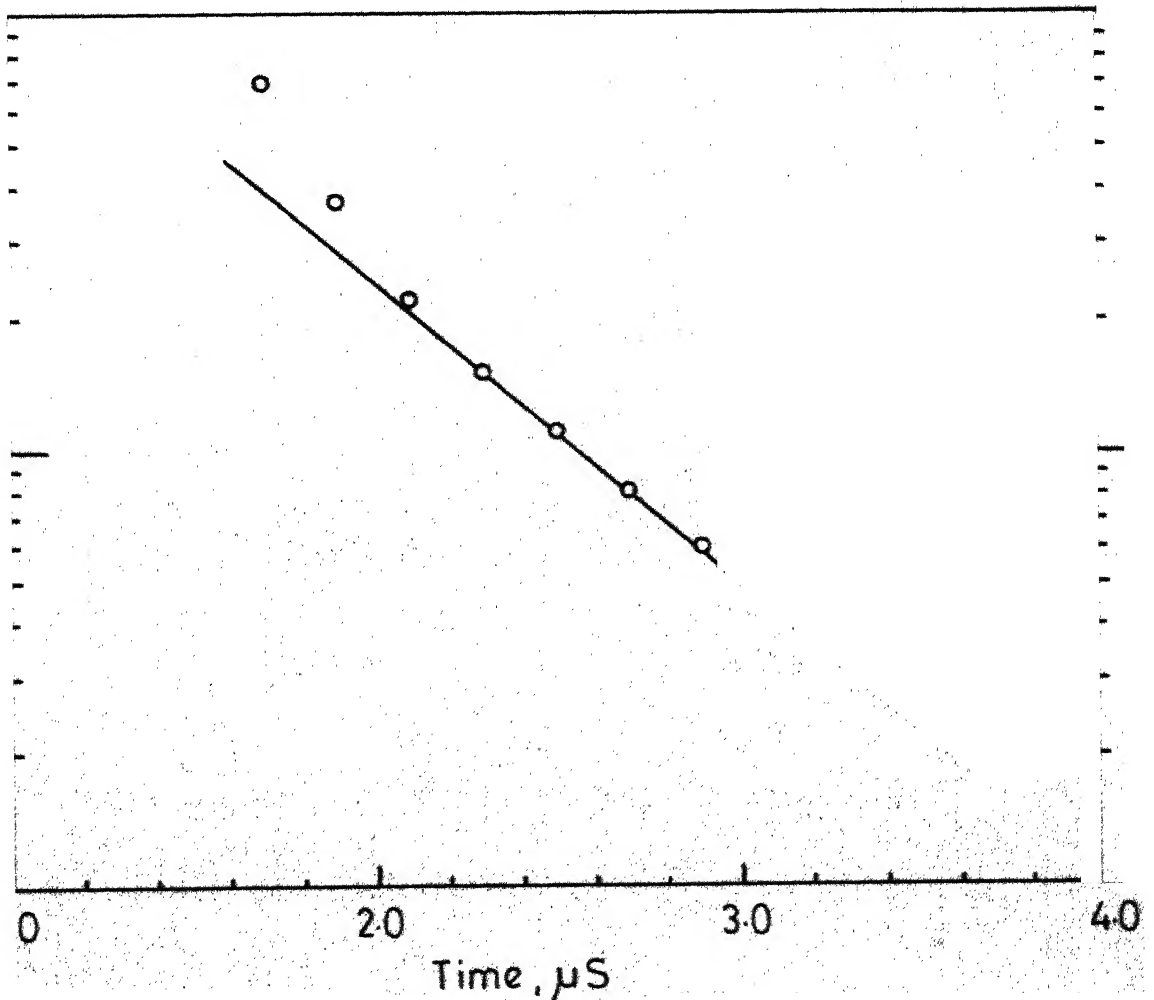
Table No. 4.6

Vibrational relaxation data in 9.5% SO_2 + He mixture

S.No.	p_1 (mmHg)	u_s (mm/μS)	T_2 (°K)	τ_L (μS)	$P\tau$ (atm. μS)
1	1.40	2.606	1605.5	0.334	0.054
2	1.73	2.338	1346.9	0.422	0.064
3	1.76	2.198	1222.8	0.640	0.084
4	1.84	2.087	1130.0	0.670	0.081
5	2.92	1.838	938.5	0.521	0.071
6	1.88	1.899	984.8	1.305	0.125
7	3.28	1.607	780.0	1.667	0.174
8	4.92	1.531	731.0	1.630	0.222
9	11.28	1.347	622.9	0.834	0.177
10	8.16	1.636	798.2	1.050	0.287
11	8.00	1.657	813.0	0.821	0.229
12	8.38	1.663	819.6	0.622	0.183
13	7.96	1.762	884.6	0.635	0.209
14	7.88	1.858	951.0	0.374	0.146
15	4.16	1.825	929.1	0.790	0.150
16	3.84	2.131	1164.4	0.374	0.099
17	4.24	1.872	960.6	1.185	0.245
18	3.72	1.952	1022.5	0.627	0.128
19	2.56	2.166	1189.5	0.374	0.069
20	1.68	2.245	1260.0	0.630	0.084
21	1.40	2.334	1340.0	0.703	0.086
22	1.20	2.459	1457.5	0.548	0.066
23	1.60	2.424	1426.6	0.530	0.082
24	1.36	2.598	1585.8	0.369	0.057

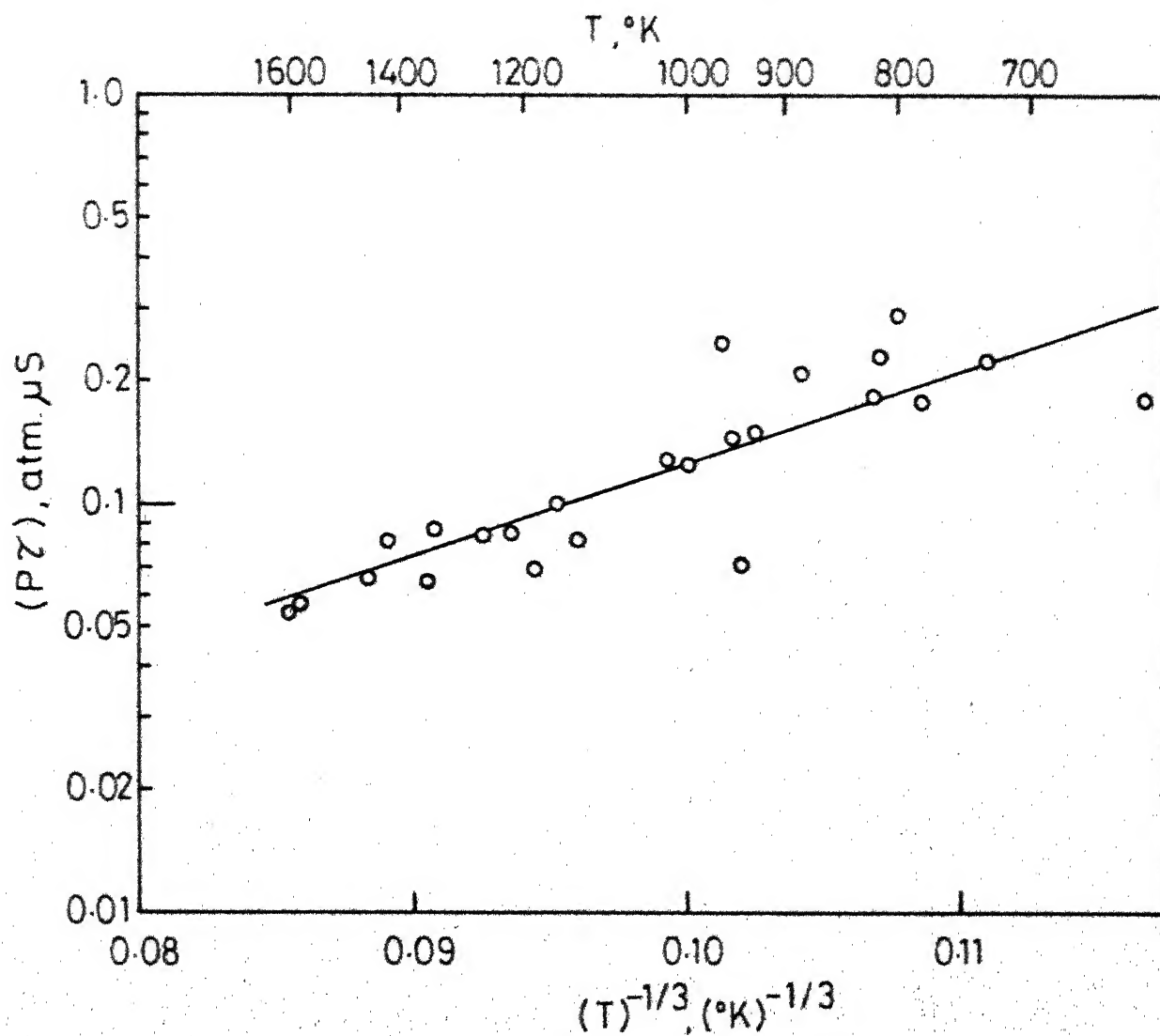Fig. 4·15 – Vibrational relaxation times in 9·5% SO_2-He mixture.

$(P\tau)_{SO_2-M}$ replaced by $(P\tau)_{SO_2-He}$. Thus for each experimental point, the value of $(P\tau)_{SO_2-He}$ is evaluated and these points are used for a least squares analysis to fit a Landau-Teller type equation. The resulting expression is

$$(P\tau)_{SO_2-He} = \exp\left[-7.58 + 54.68\ T^{-1/3}\right]; \quad \sigma = 32.2\%$$

The solid line of fig.(4.15) is obtained from the mixture rule with X = 0.095 and using eqs.(4.8) and (4.20) for $(P\tau)_{SO_2-SO_2}$ and $(P\tau)_{SO_2-He}$ respectively. The results of the present work are compared with the lone value of the slower rate of laser fluorescence studies[22] at room temperature, as shown in fig.(4.16). The solid line is given by eq.(4.20) and the dashed line is its extrapolation to room temperature. The error bars given in fig.(4.16) correspond to the standard deviation given above. It can be seen that the present results compare favourably with the value from Ref. 22.
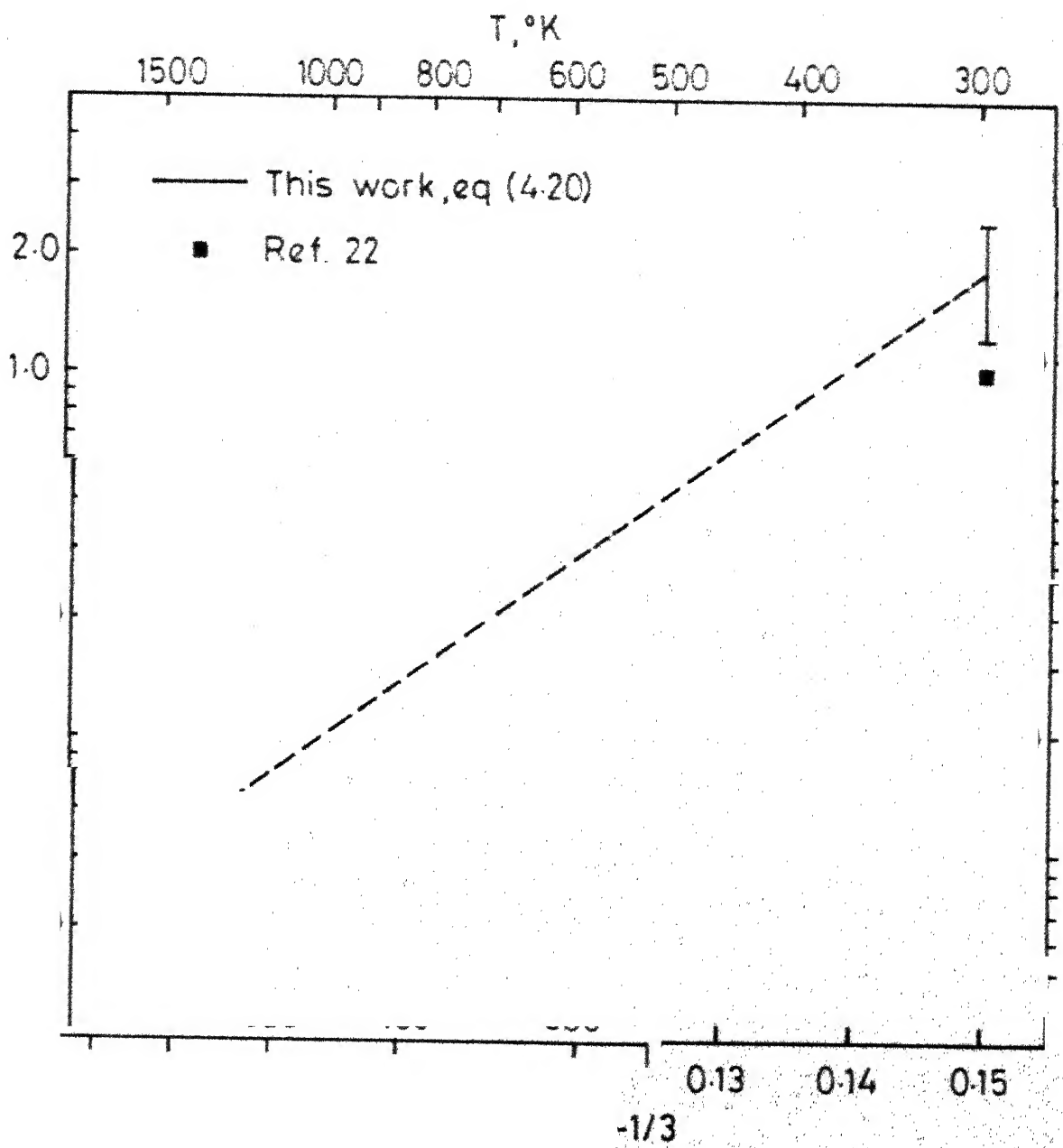
Fig. 4.1 – Vibrational relaxation times in 9.5% SO_2–He mixture.

CHAPTER - V

CONCLUSIONS

Vibrational relaxation in SO_2, SO_2-Ar and SO_2-He systems is studied by means of a shock tube laser schlieren technique over a wide temperature range. Density gradient profiles in these systems show a double exponential behaviour. This finding, consistent with the earlier ultrasonic studies, is understood to be due to the presence of a slow V-V step involved in the relaxation of SO_2 vibrational levels. The longer relaxation times obtained in the present study are identified with this slower rate.

The relaxation times in pure SO_2 are obtained in the temperature range of 550°K - 1200°K. The relaxation times in SO_2-Ar system are measured at three compositions - 11% SO_2, 20% SO_2 and 54% SO_2 in Argon. The temperature range covered for these compositions is 700°K - 2100°K. From these measurements $(P\tau)_{SO_2-SO_2}$ and $(P\tau)_{SO_2-Ar}$ are obtained in the same temperature range. Similarly $(P\tau)_{SO_2-He}$ is obtained from measurements made on a 9.5% SO_2-He mixture in the temperature range 700°K - 1600°K.

The values obtained in the present study agree well with the earlier ultrasonic and laser induced fluorescence

studies which covered a range of 300°K - 1100°K.

The measured relaxation times in SO_2 are found to have a weak temperature dependence in the temperature range studied.

The efficiency of a collision partner in exciting the stretching modes in SO_2 is found to be in the order of $Ar < SO_2 < He$.

REFERENCES

1. K.F. Herzfeld & T.A. Litovitz, <u>Absorption and dispersion of ultrasonic waves</u>, Academic press, New York, 1959.

2. T.L. Cottrell and J.C. Mc Coubrey, <u>Molecular energy transfer in gases</u>, Butterworth, London, 1961.

3. L.O. Hocker, M.A. Kovaes, C.K. Rhodes, G.W. Flynn and A. Javan, Phys. Rev. Letters <u>17</u>, 233 (1966).

4. C.B. Moore, <u>Adv. in Chem.Phys.</u>(edited by I. Prigogine and S.A. Pice, John Wiley and sons,Inc., New York, 1973)Vol.23.

5. A.G. Gaydon and I.R. Hurle, <u>The shock tube in high temperature chemical physics</u>, Reinhold Publishing Corp., New York, 1963.

6. G.M. Burnett and A.M. North, Eds. <u>Transfer and storage of Energy by Molecules</u>, Vol. 2 vibrational energy (Wiley Interscience, London, 1969).

7. J.H. Kiefer and R.W. Lutz, J.Chem. Phys., <u>44</u>, 658 (1966).

8. W.D. Breshears and P.F. Bird, J.Chem.Phys.,<u>50</u> , 333(1969).

9. C.J.S.M. Simpson and T.R.D. Chandler, J.Chem.Phys., <u>51</u>, 2214 (1969).

10. W.D. Breshears and L.S. Blair, J.Chem.Phys., <u>59</u>, 5824(1973).

11. W.D. Breshears, P.F. Bird and J.H. Kiefer, J.Chem.Phys., <u>55</u>, 4017 (1971).

12. J.H. Kiefer, J.Chem.Phys., <u>61</u>, 244 (1974).

13. J.F. Bott, J.Chem.Phys., <u>57</u>, 96 (1972).

14. J.D. Lambert & R.Salter, Proc. Roy. Soc.(Lond.) <u>A 243</u>, 78 (1957).

15. J.C. Mc Coubrey, R.C. Milward and A.R. Ubbelohde, Proc. Roy. Soc. (Lond.) <u>A 264</u>, 299 (1961).

16. F.D. Shields, J.Chem.Phys., <u>46</u>, 1063 (1967).

17. F.D. Shields and B. Anderson, J.Chem.Phys., <u>55</u>, 2636(1971).

18. H.E. Bass, T.G. Winter and L.B. Evans, J.Chem.Phys., $\underline{54}$, 644 (1971).

19. P.G. Dickens and J.W. Linnett, Proc. Roy. Soc.(Lond.) $\underline{A\ 243}$, 84 (1957).

20. J.D. Lambert, D.G. Parks-Smith and J.L. Stretton, Trans. Faraday Soc. $\underline{66}$, 2720 (1970).

21. D.R. Siebert, F.R. Graliner and G.W. Flynn, J,Chem.Phys., $\underline{60}$, 1564 (1974).

22. D.R. Siebert and G.W. Flynn, J.Chem.Phys., $\underline{62}$, 1212,(1975).

23. B.L. Earl, A.M. Ronn and G.W. Flynn, Chemical Physics, $\underline{9}$, 307 (1975).

24. L.Landau and E. Teller, Phys. Z. Soviet, $\underline{10}$, 34(1936).

25. F.I. Tanczor, J.Chem.Phys., $\underline{25}$, 439 (1956).

26. R.N. Schwartz, Z.I. Slawsky and K.F. Herzfeld, J.Chem. Phys. $\underline{20}$, 1591 (1952).

27. E.L. Resler and M. Scheibe, J. Acoust. Soc. Am. $\underline{27}$, 932 (1955).

28. J.H. Kiefer and R.W. Lutz, Phys. Fluids $\underline{8}$, 1393 (1965).

29. V.Blackman, J.Fluid Mech., $\underline{1}$, 61 (1956).

30. P. A. Blythe, J, Fluid Mech. $\underline{10}$, 33 (1961).

31. N.H. Johannesen, J. Fluid Mech. $\underline{10}$, 25 (1961).

32. R.W. Lutz and J.H. Kiefer, Phys. Fluids,$\underline{9}$, 1638 (1966).

33. V.V.N. Kishore, M.Tech. thesis, Jan. 1973.

34. V.V.N. Kishore, K.M.S. Prasad and V.Subba Rao, to be published in the J. Aero. Soc. India, Aug. 1976 issue.

35. H. Shin, J. Amer. Chem. Soc., $\underline{90}$, 3029 (1968).